Journal of Marine Technology and Environment

Vol. I, year 2014

ISSN 1844-6116

YEAR VII, 1/2014
ISSN 1844 – 6116

JOURNAL OF MARINE TECHNOLOGY AND ENVIRONMENT

This Journal has been founded in 2008 as a biannual publication of
Constanta Maritime University/ROMANIA

TOPICS

- Marine Science and Engineering
- Marine Environmental Issues
- Marine Renewable Energy and Sustainability
- Maritime Safety
- Marine Chemistry
- Marine Corrosion and Material Science
- Ship Design, Building Technologies
- Ocean Engineering
- Advanced Technologies for MET
- Advances in numerical methods for marine engineering
- Algorithms for multidisciplinary problems in marine engineering
- Other related topics

JOURNAL ADDRESS
Journal of Marine Technology and Environment
Constanta Maritime University, 104, Mircea cel Batran Street, 900663, Constanta, Romania
Tel: +40 241 664 740/ 107
Fax: +40 241 617 260
E-mail: jmte@imc.ro
http://cmu-edu.eu/jmte/

EDITURA NAUTICA
Constanta Maritime University
Constanta Maritime University, 104, Mircea Cel Batran Street, 900663, Constanta, Romania

CONTENTS

1. **CONSIDERATIONS REGARDING THE IMPACT OF SHIP INTACT STABILITY LOSS ON MARINE POLLUTION**
[1]ANDREI CRISTIAN, [2]LAMBA MARINEL-DANUT, [3]HANZU-PAZARA RADU, [4]BLAGOVEST BELEV
[1,2,3]Constanta Maritime University, Romania, [4]Naval Academy "N.Y.Vaptsarov" -Varna, Bulgaria …… 7

2. **PRINTED THICK FILM HEATING ELEMENTS FOR USE IN SHIPS**
APRAHAMIAN BOHOS
Technical University of Varna, Bulgaria…… 17

3. **NEW TRENDS IN THE CONTENT ON THE BULGARIAN NAUTICAL NAVIGATION CHARTS**
DACHEV YURIY
"Nikola Vaptsarov" Naval Academy - Varna, Bulgaria…….. 25

4. **QUANTUM DOTS INTERACTION WITH PROKARYOTES INVOLVED IN THE MARINE BIOREMEDIATION PROCESS**
[1]GHITA SIMONA, [2]SARCHIZIAN IRIS
[1]Constanta Maritime University, [2]County School Inspectorate of Constanta, Mihai Eminescu no. 11, Romania…….. 29

5. **AUTOMATED AND MECHANICAL EQUIPMENT FOR COLLECTING OF METEOROLOGICAL INFORMATION ON BOARD OF THE SHIP**
GRANCHAROV IVAYLO
"Nikola Vaptsarov" Naval Academy, Varna, Bulgaria…… 35

6. **NEW TECHNOLOGIES USED FOR AUTOMATION OF CONTAINER HANDLING AT TERMINALS**
GRANCHAROVA VALENTINA
"Nikola Vaptsarov" Naval Academy, Varna, Bulgaria…… 41

7. **ANALYSIS OF SHIP OPERATION FOR A CONTAINER TERMINAL**
[1]LOKE K.B., [2]A.H. SAHARUDDIN, [3]A.R. IBRAHIM, [4]I. RIZAL, [5]A.S.A. KADER, [6]A.M. ZAMANI
[1,2,3,4,5,6]School Of Maritime Business And Management Universiti Malaysia Terengganu, Malaysia…… 49

8. **CONSIDERATIONS ON THE PERFORMANCE OF SINGLE VAPOR COMPRESSION CYCLES WITH SUPERHEATING AND WITHOUT SUBCOOLING**
MEMET FEIZA
Constanta Maritime University, Romania…… 57

9. **THE ASSESSMENT OF CONVECTIVE COEFFICIENT OF HEAT TRANSFER IN EVAPORATORS WORKING WITH R 134a, USING KANDIKLAR EQUATIONS**
MITU DANIELA - ELENA
Constanta Maritime University,Romania..... 63

10. **THE ANALYSIS OF SHORT-CIRCUIT CURRENTS IN A NAVAL ELECTRICAL NETWORK BY MEANS OF SOFTWARE TOOLS**
[1]SAMOILESCU GHEORGHE, [2]MARIN GEORGIANA
[1]"Mircea cel Batran" Naval Academy, [2]Reseach Center for Navy, Romania…. 71

11. **ECOTOXICOLOGICAL ASSESSMENT IN SOME POINTS OF THE ROMANIAN BLACK SEA COASTAL ZONE**
SUNDRI MIRELA – IULIANA
Constanta Maritime University, Romania..... 79

CONSIDERATIONS REGARDING THE IMPACT OF SHIP INTACT STABILITY LOSS ON MARINE POLLUTION

[1]ANDREI CRISTIAN, [2]LAMBA MARINEL - DANUT, [3]HANZU - PAZARA RADU, [4]BLAGOVEST BELEV

[1,2,3]Constanta Maritime University, Romania, [4]Naval Academy "N.Y.Vaptsarov"-Varna, Bulgaria

The article presents very important aspects of marine pollution generated by the loss of intact ship stability. Based on the statistics issued by maritime organizations, it is presented the correlation between loss of ships intact stability and the hull structural failure, being revealed that the first can be considered as a primary event in certain accidents of marine pollution. Moreover, the paper illustrates correlation between loss of intact ship stability and pollution of marine environment not only by oil but also by harmful substances contained in bulk cargo transported on board ships and accidentally discharged into the sea due to ship stability failure.

***Keywords**:* marine, oil, pollution, stability

1. INTRODUCTION

Despite the efforts of maritime organizations, accidents involving marine pollution from ships will continue to occur. There are many types of pollutions generated from ships, among can be mentioned oil, chemicals, garbage, marine pests from ship's ballast, air pollution or anti-fouling paint used for the ship's hull. Marine pollution, through oil spills or discharged of harmful substances from ships, have a significant impact on marine ecosystems by causing contamination, toxic effects or long-term impacts.

One type of the accident, involving such consequences and with a degree of risk that have to be assessed rationally is the loss of ship's intact stability. In the situations of pollution events caused by ships, intact or damage stability is an important factor which is playing an important role. In this respect, a question may arise on how much is the impact of ship stability loss on marine pollution? The first part of the answer of this question may be revealed by the records and statistics of the incidents involved marine pollution due to loss of ship stability. The second part of the answer may be revealed by the particularities of ships and cargo transported.

The analysis in this paper is carried out considering the loss of ship stability as the primary event of marine pollution and not as a link in a chain of events where primary cause is, for instance, fire, grounding or collision.

Moreover, the type of pollution that is taken into consideration is not only the pollution resulted from the spillage of oil (either as cargo transported by tanker ships or as bunker used by all kinds of ships) but also as a result of accidentally discharging of the cargo transported (other than oil) that may cause a potential pollution to marine environment.

2. STATISTICS OF ACCIDENTS INVOLVING MARINE OIL POLLUTION

Statistics are indispensable factors for the amelioration of safety of ships as well as protection of marine environment. Through the reconciliation of accidents that may appear isolated to interested parties, they permit tracking of typical causes of accidents; conversely, they can prevent, after a serious accident due to some fortuitous cause, the taking of incautious measures under the pressure of public opinion, which always inclines to gauge the gravity of the causes by that of the results. Lastly, they permit appraisal of the efficacy of rules in force.

One of the most accurate statistics regarding incidents of oil spills generated by tanker ships are provided by the International Tanker owners Pollution Federation (Figure1).

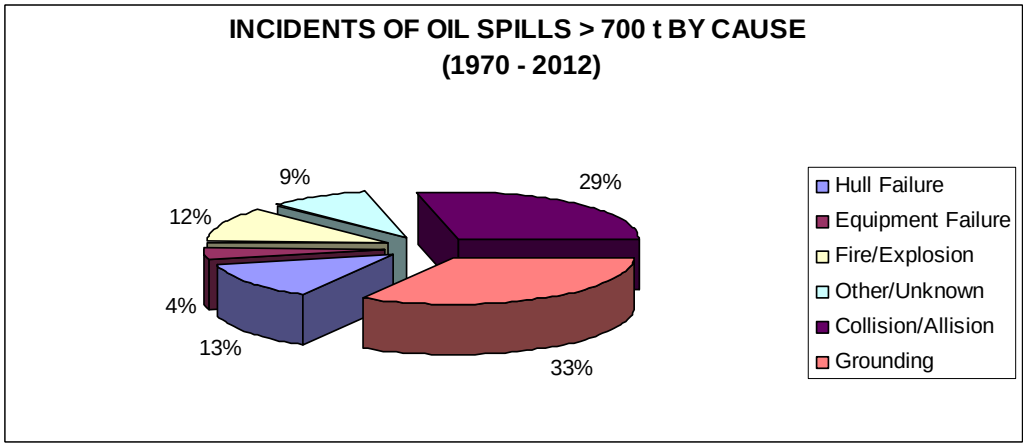

Figure 1. Incidence of spills > 700 tonnes by cause, 1970-2012 [15]

The graph presented in Figure 1 is illustrating the incidence of oil spills based on the primary cause of the spill. As can be noted, the statistic not includes a category of incidents of marine pollution having the primary cause the loss of ships intact stability.

However, it is revealed the fact that some incidents are categorized as “Other/Unknown”. In this category, it can be assumed that the primary cause of oil spill is unknown or the incidents were based on other causes less frequent to tanker ships like for example loss of intact stability. In order to establish this aspect, it is necessary to study the investigation reports for each accident.

3. ACCIDENTS INVOLVING MARINE OIL POLLUTION

In the statistics presented, in the category “Hull Failure” can be introduced, in our opinion, the situations when the ship stability was lost and was the primary cause of hull failure followed by the broke of ships and in the end by oil spillage. Based on this assumption, in this category can be introduced two of the most significant accidents in this respect, as follows:

- ***MT Erika***

The oil tanker Erika, loaded with about 30,000 tonnes of heavy fuel, encounter heavy weather conditions, on 11th December 1999, about 60 nm off the coast of Brittany in

Northwest France. The vessel broke in two and an estimated 20,000 tonnes of cargo was lost to the sea [4].

- ***MT Prestige***

On 15th November 2002, the oil tanker Prestige broke in two and sank as a result of burst one of its twelve tanks during stormy weather conditions about 140 nm west of Vigo, Spain. An estimated quantity of 63,000 tonnes of oil was lost into the marine environment [4].

However, the marine environment is not polluted only due to oil spills from the cargo transported on board tanker ships as a consequence of type of accidents presented above. This kind of accidents (structural failure) can lead to pollution of marine environment by the fuel oil used as bunkers on board of all kind of ships. In this respect, one of the relevant accidents is the one presented below:

- ***MV MOL Comfort***

On 17th June 2013, while en route from Far East to Northern Europe, the containership encountered a severe storm in Indian Ocean and broke in two. It was estimated that a considerable amount of bunker (fuel oil) was accidentally spilled into the ocean [16].

4. LOSS OF SHIP STABILITY AS PRIMARY EVENT OF MARINE POLLUTION GENERATED BY HULL FAILURE

Based on the accidents presented above, we can affirm that loss of ship stability in severe sea conditions is the primary cause of marine oil pollution due to structural failure of ship's hull.

The loss of ship stability in severe sea conditions which leads to structural failure (broke the ship in two separate parts) can be attributed to development of excessive stresses due to variations of righting moment on waves generated by high rolling angles.

The alterations of the righting lever, which can be expressed by the differences of the righting levers at the trough and crest condition, are always related to a specific hull form, and resulting in significant changes of hull's wetted surface and waterline area (Figure 2 and Figure 3).

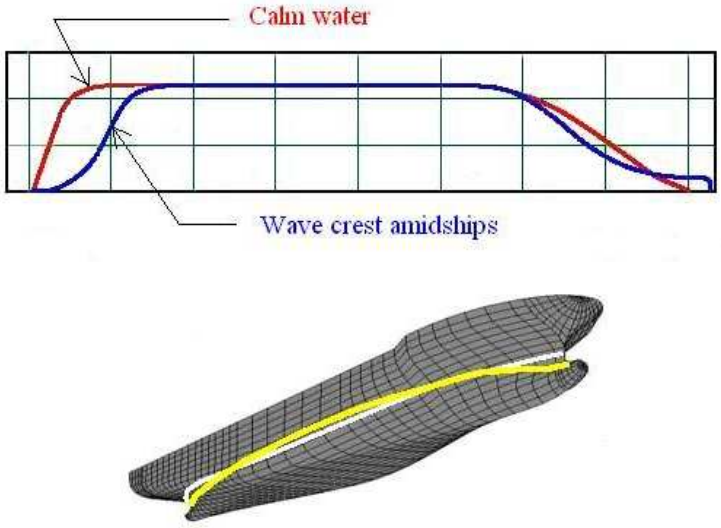

Figure 2. Change of ship's waterplane area on wave crest

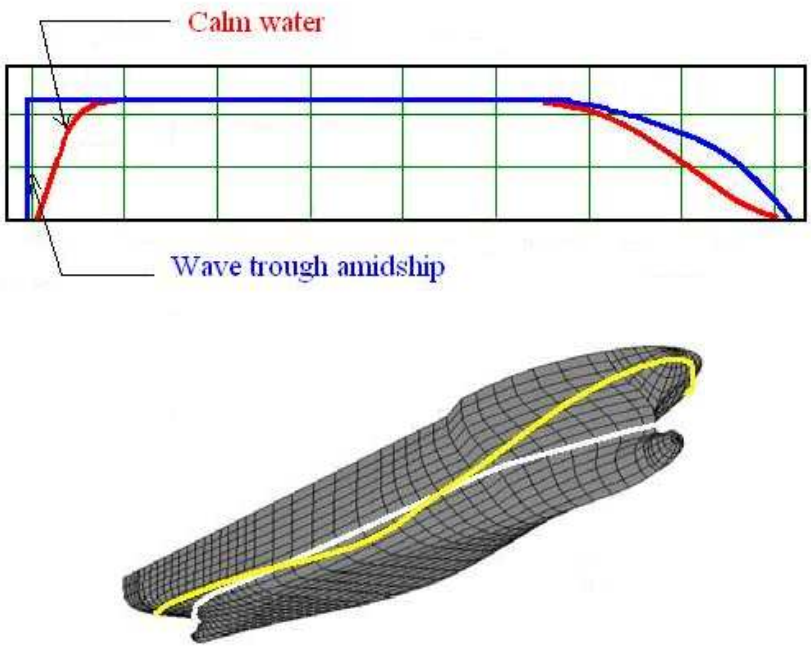

Figure 3. Change of ship's waterplane area on wave trough

The energy introduced into a specific hull form in a sea state may be expressed by the alterations of the area below the righting levers at crest and trough condition. The calculation and representation of righting lever curves for a ship, in wave situations, where the wave crest is situated amidship and where the ship's midship section is situated in a wave trough is illustrated in Figure 4.

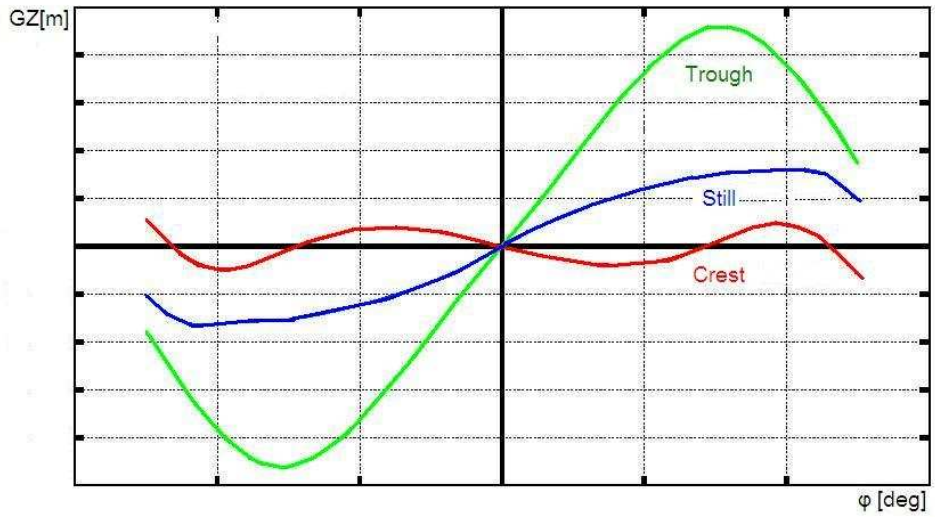

Figure 4. Resulting righting lever arm curves due to position of ship on wave

It is revealed that the significant changes in ship's stability due to alterations of righting levers and thus the ship loose the stability almost completely when on wave crest. In the crest condition, the aft body is significantly out of water which results in significant loss of stability. In the trough condition, the ship has excessive stability due to the high form stability of the fore body.

The righting levers oscillate periodically between the extreme values of the lever arms used for calculations. When the stability loss on the crest exceeds a certain limit, the vessel may have no stability left at all and capsize if it rest in this crest condition for a certain time (this is a typical situation of pure loss of stability).

If the stability remains at a low level, for a sufficient long time, there is a danger that high stresses, such as bending moments and shearing forces, are developed in ship's structure, due to variation of buoyancy force (given by the red arrow) and displacement force (given by the blue arrow) acting on the ship's hull (Figure 5 and Figure 6). In this situation, the successive and rapid alterations between sagging and hogging of hull usually lead to extended cracks in ship's hull followed by broken of ship in separate parts.

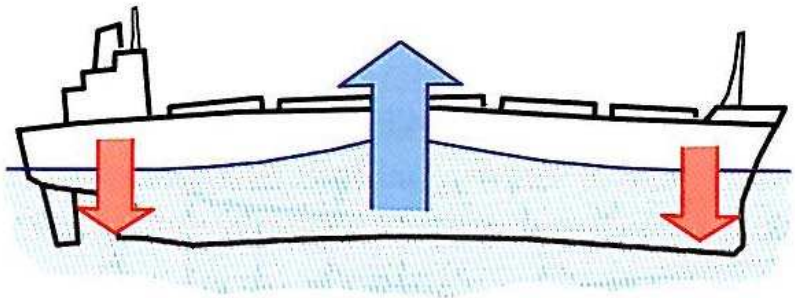

Figure 5. Hogging moments increased due to excess buoyancy by the wave crest amidships [2]

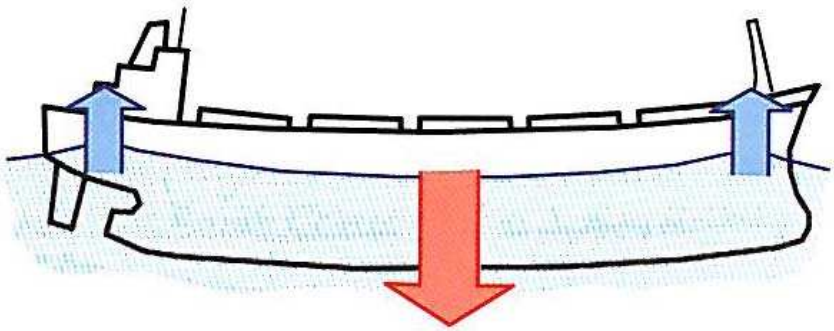

Figure 6. Sagging moments increased due to less buoyancy by the wave through amidships [2]

It is important to be mentioned that a major spill of crude oil from an oil tanker may do less damage to the marine environment than a spill of bunker oil from a cargo ship, as bunker oil is more toxic than crude oil and is more difficult to clean [1].

IMO by the Sub-Committee on Flag State Implementation (FSI), using the data received from rescue Co-ordination Centers (RCCs) in the form of situation reports (SITREPs) and

other sources, prepare one of the most appropriate statistics to maritime casualties [9], [10], [11], [12], [13], [14].

According to IMO, principal casualties are divided into listing, capsizing, grounding/stranding, collision, hull/structural failure, fire/explosion and machinery damage. Is the only one statistic where listing and capsizing casualty are counted as separate category.

The graphic from the Figure 7, gives a general overview about the total casualties occurred in the whole reference period, for all types of ships.

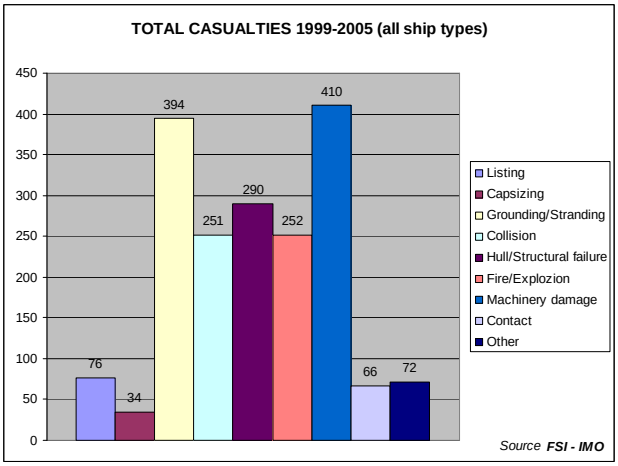

Figure 7. Total number of casualties for period 1999-2005 for all ship types [9]

From the statistic presented in Figure 7 can be noted that the category of “Hull/Structural Failure” accidents has an important share, with an important number of ships that suffered from such type of accident.

Moreover, the statistic presented in Figure 8, revealed the types of ship’s that suffered such an accident. In this way, it can be noted that the number of tanker ships is relatively high and not to be left away.

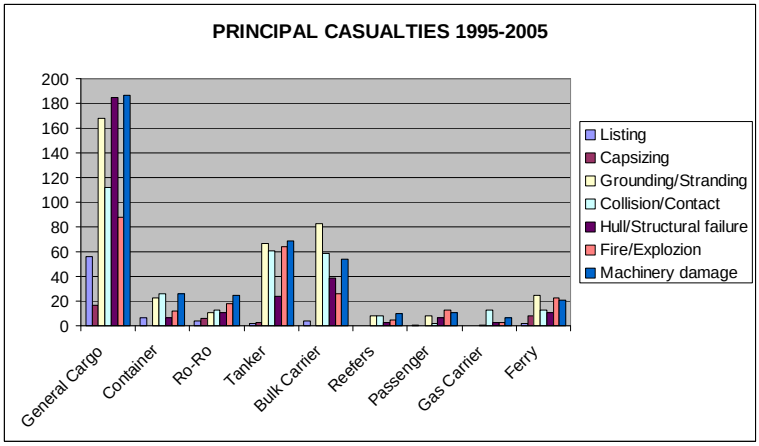

Figure 8. Total number of casualties for period 1999-2005 for principal casualties [9]

Once the double hull design of ships (especially for tanker ships) was introduced, it was believed that the overall structural integrity of the vessel has been increased. As per graph presented in Figure 9, it can be noted that incidents related to "Seaworthiness" (which in our opinion includes structural failure and intact stability because as per seaworthiness concept in shipping this means " *a vessel must be tight, staunch, strong and in every way fit for the voyage"*) are affecting in a large amount also the double hull tanker ships.

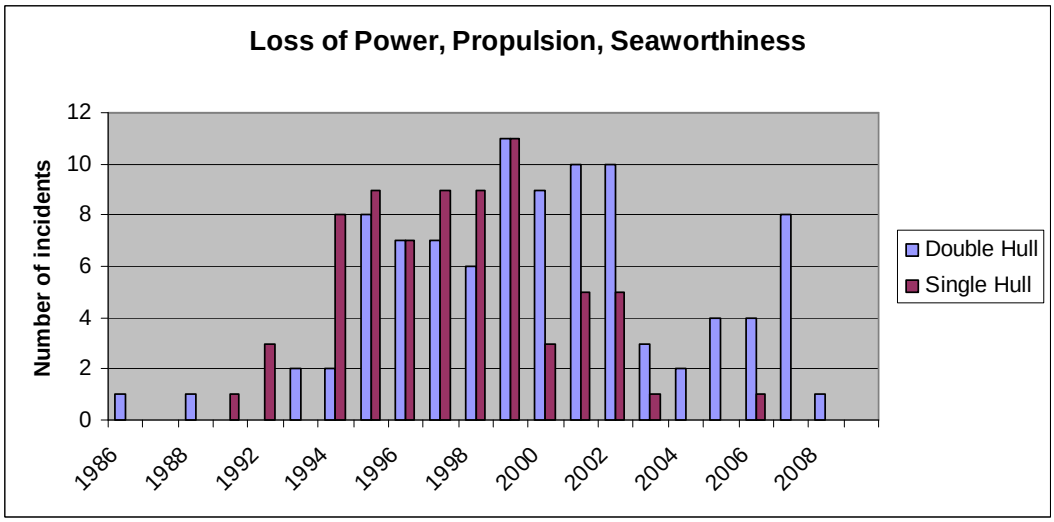

Figure 9. Number of tanker Loss of Power, Propulsion, Seaworthiness, in Washington State, from 1986-2008 [5]

The increased number of incidents for double hull is because an increased effect of hull stress and structural fatigue on double hulls. Due to the fact that in double hull tanker ship the distribution of cargo and ballast over the ship is uniform (compared to a single hull tanker ship where ballast tanks can be positioned to minimize longitudinal bending and shear stresses), accurate stress prediction is more complicated. Many of the increased cruciform joints, where primary structural members terminate on double skin, are located in areas where high stress levels and potential stress concentration features may lead to failure of structure [5].

A ship constructed in double hull tends to be stiffer than a ship constructed in single hull and this can the affect local stresses induced by operational loads as well as the residual stresses induced during construction [17]. In this respect, it is obvious that ships constructed in a double hull design will operate with an increased stress levels than ship constructed in single hull design. Higher stresses will generate the increasing risk of buckling failure and this risk will increase during entire life of the vessel if is taken into consideration the loss of plate thickness caused by corrosion [5]. Moreover, the higher stresses can also generate an increased likelihood of developing small fatigue cracks [18].

Having in view the aspects presented here, we consider that the roots of structural failure and high stresses loads (which are the main causes of an accidental pollution) are in the loss or decreasing the ship intact stability when the vessel is encountering severe sea conditions.

5. LOSS OF SHIP STABILITY AS PRIMARY EVENT OF MARINE POLLUTION GENERATED BY PROPRIETIES OF CARGO CARRIED

Another factor involved in marine pollution due to loss of ship intact stability is the pollution generated by harmful proprieties of cargo discharged into the sea due to ship's capsizing.

One of the most dangerous phenomenon that lead to loss of ship stability and finally to ship capsize is the shifting of bulk cargoes due to liquefaction process.

Many alarms was raised [6], [7], in relation with the severe consequences of the bulk cargoes liquefaction on board vessels over safety and stability of ships.

Over the recent years, an increased number of vessels lost their intact stability due to bulk cargo liquefaction. Part of them developed large angles of list whilst others unfortunately capsized. The below table illustrate the casualties happened in the last decade that involved severe ship stability failure, like capsizing, due to cargo liquefaction, as stated in [3].

Table 1. Casualties of ship stability failures related to liquefaction of cargo (Class NK, 2012)

Date of incident	Vessel	Cargo loaded	Type of incident	Location
1988	Mega Taurus	Nickel ore	Capsize	Indonesia
1998	Sea prospect	Nickel Ore	Capsize	Indonesia
18/05/2005	Hui Long	11,245 tons of Fluorspar	Capsize	West of Sri Lanka
08/2009	Hodasco 15	6,000 tons of Iron ore	Capsize	Malaysia
09/09/2009	Black Rose	23,000 tons of Iron ore	Capsize	Few miles out of Paradip port (India)
17/07/2009	Asian Forest	13,000 tons of Iron ore	Capsize	Mangalore (India)
21/10/2010	Jian Fu Star	43,000 tons of Nickel ore	Capsize	West of Taiwan
10/11/2010	Nasco Diamond	55,150 tons Nickel ore	Capsize	East of Taiwan
03/12/2010	Hong Wei	40,000 tons Nickel ore	Capsize	South of Taiwan
21/11/2011	Bright Ruby	25,000 tons Iron ore	Capsize	South of Taiwan
25/12/2011	Vinalines Queen	54,000t nickel	Capsize	South China Sea
14/08/2013	Trans Summer	55,000 tons nickel ore	Capsize	South China Sea
17/12/2013	Harita Bauxite	50,000 tons nickel ore	Capsize	South China Sea

The most significant consequence for the vessel, resulting from liquefaction, is cargo shift, cargo flow to one side of the ship with a roll one way but not completely return with a roll the other way, progressively leading to loss of stability (Figure 10). This may produce dangerous angles of list and in some instances the resulting loss of stability can be such as the vessel capsizes.

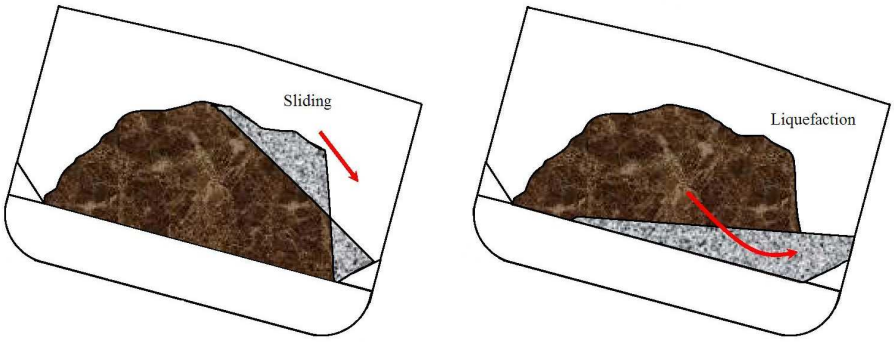

Figure 10. Developing of list due to cargo liquefaction

As a consequence of capsize and sinking of the vessel is the pollution of marine environment generated by the accidentally discharging into the sea of the bulk cargo transported. Thousands of tons of cargo, such as iron ore, nickel ore, fluorspan or bauxite with harmful components for the marine environment, as described in the IMO IMSBC Code 2008 [8], are discharged into the sea.

Apart from the harmful substances contained in the cargo, the marine environment is polluted by the oils used on board as bunkers (fuel oil, diesel oil, lubricating oil).

Based on the analysis presented it can be affirmed that a new type of pollution the marine environment has been approached. Having in view the large quantities of cargo, that contains harmfull substances for marine environment, carried by bulk carrier ships and are accidentally discharged into the sea due to sinking of ships, it can have a dangerous impact on zones having high ecological quality.

6. CONCLUSIONS

The present paper has considered the aspects of marine pollution in relation with intact ship stability loss. Based on the analysis of statistics, issued by different maritime organizations, it was revealed the fact that an event such “Hull/Structural failure” (which is considered as a primary event in marine oil pollution by tanker ships) is in fact the result of ship intact stability loss.

Thus, loss of intact ship stability can be considered as a primary event in the accidents involving marine pollution not only by oil (as cargo from tanker ships or as bunker fuel for other types of ships) but also by harmful substances contained in different types of bulk cargo carried on board bulk carrier ships.

A thorough understanding and correlation of ship intact stability and structure of the hull can be an essential matter for the safety of ship and marine environment.

REFERENCES

[1]. Australian Marine Environment protection Association - ***Ships and Marine Environment, Types of Pollution***, 2014, On line at: http://www.ausmepa.org.au/ships-and-the-marine-environment/5/types-of-pollution.htm.

[2]. Clark I. C., - ***Stability, Trim and Strength for Merchant Ships and Fishing Vessels***, Second Edition, The Nautical Institute, London, 2008.

[3]. Class NK - ***Guidelines for the Safe Carriage of Nickel Ore***, First Edition, Nippon Kaiji Kyokay, Tokyo,2012.

[4]. European Maritime Safety Agency - ***Operational tasks, Satellite oil Spill Monitoring (CleanSeaNet)***, 2014, On line at: http://emsa.europa.eu/operations/cleanseanet/122-cleanseanet/479-deliberate-discharges.html.
[5]. Elise DeCola Nuka Research & Planning Group, LLC. - ***A Review of Double Hull Tanker Oil Spill Prevention Consideration***, Report to Prince William Sound RCAC, Alaska, 2009.
[6]. Gard - ***Loss prevention Circular No.06-11 Cargo liquefaction problems – sinter feed from Brazil***, May 2011.
[7]. Gard News 197 - ***Liquefaction of unprocessed mineral ores – Iron ores and nickel ores***, February/April 2010.
[8]. IMO Resolution MSC.268(85) - ***Adoption of the International Maritime Solid Bulk Cargoes (IMSBC) Code***, London 2008.
[9]. IMO FSI.3/Circ.1 - ***Casualty statistics and investigations. Very serious and serious casualties for the year 1998***, London 1999.
[10]. IMO FSI.3/Circ.2 - ***Casualty statistics and investigations. Very serious and serious casualties for the year 1999***, London, 2001.
[11]. IMO FSI.3/Circ.3 - ***Casualty statistics and investigations. Very serious and serious casualties for the year 2000***, London, 2002.
[12]. IMO FSI.3/Circ.4 - ***Casualty statistics and investigations. Very serious and serious casualties for the year 2001***, London, 2004.
[13]. IMO FSI.3/Circ.5 - ***Casualty statistics and investigations. Very serious and serious casualties for the year 2002,*** London, 2005.
[14]. IMO FSI.3/Circ.6 - ***Casualty statistics and investigations. Very serious and serious casualties for the year 2003***, London, 2005.
[15]. International Tanker Owners Pollution Federation - ***Oil Tanker Spill Statistics 2012***, Impact PR & Design Ltd, Canterbury, UK, 2012.
[16]. Maritime Bulletin - ***Accidents***, 2013, On line at: http://www.news.odin.tc/index.php?page=view/article/513/MOL-Comfort-broke-in-two-and-sank-in-Arabian-sea.
[17]. National Research Council - ***Double Hull Tanker Legislation: An Assessment of The Oil Pollution Act of 1990***, National Academy Press, Washington, D.C., 1999.
[18]. Oil Companies International Marine Forum - ***"Double Hull Tankers: Are they the Answer?"***, On line at: http://www.ceida.org/prestige/Documentacion/dobrecascopetroleiros.pdf

PRINTED THICK FILM HEATING ELEMENTS FOR USE IN SHIPS

APRAHAMIAN BOHOS

Technical University of Varna, Bulgaria

The paper presents our work in developing printed thick film heater elements on ceramic substrates for heating in the range of 300 – 400 ^{o}C. Two types of samples are realized and experimentally investigated. Their leakage currents are measured and their resistance to the sea mist impact is checked. The heater elements on ceramic substrates are considered promising for application in ships.

***Keywords**:* heating element, screen printing, printed thick film, thick film ink, leakage current

1. INTRODUCTION

In ship heating systems, the most commonly seen heating element is the tubular kind. This is because these particular devices are relatively inexpensive, when compared to cartridge and other heater types, and are reliable. Whether single- or double-ended, they are designed to be used in both radiant and contact surface heaters. The element itself can even be formed into custom shapes for various applications, e.g. the ship immersion heaters consist of tubular elements in a threaded hex plug. They screw directly through threaded openings in tank walls to heat liquids, viscous fluids, forced air, and gases by direct contact (http://www.nauticexpo.com/boat-manufacturer/immersion-heater-ships-21998.html, February 2014) ,(http://www.indeeco.com/Indeeco_C21_1_reduced.pdf, February 2014).

On other hand the International Convention for the Safety of Life at Sea, 1974 (SOLAS) requires navigating appliances and equipment to conform with appropriate performance standards not less than those adopted by the International Maritime organization (IMO). The tubular element heated systems have a few disadvantages that must be taken into consideration before being selected for installation (http://www.ehow.com/list_7699984_disadvantages-tubular-heating-elements.html, February 2014):

- There are countless models of heaters that use tubular elements, each of them utilizing a unique shape, size and pattern of bends. Due to the complex design it can be difficult to find a heating element that is exactly matched to a single heating system.
- In some heating systems the tubular elements are non-removable and cannot be replaced if it breaks down or melts. In such cases, the system must be replaced entirely at great costs.
- Tubular element heaters designed for use in submerged or underwater conditions are especially susceptible to overheating if any air manages to become trapped in the system. This pocket of dead air then causes the element to overheat and melt, which is called a "dry fire."

- In many cases, the tubular element is usually in direct contact with the medium to be heated. If the substance flowing over the element is impure, such as water, this can result in calcium or other chemical deposits forming over it corrosion if the pH value is too low or acidic.

Foil heater elements have recently been widely applied in comercial and household heaters for low temperature heating. At present heater elements with insulating substrates of polyvinylchloride, polyethylene, polyester, polyimide, silicone, etc. are mainly used (http://www.tempco.com/Catalog/Section%209-pdf/Thick%20Film.pdf, February 2014).

Their main drawback is their low operating temperature – up to 200 ^{o}C.

Having experience in developing and implementation of foil heater elements in production we faced the problem of developing heater elements for heating in the range of 300 – 400 ^{o}C for use in ships.

2. DESCRIPTION OF THE SAMPLES AND TECHNOLOGY AND APPARATUS FOR THEIR PRODUCTION

Having analized a lot of dielectrics avaible we found Al_2O_3 ceramics to be the most suitable one for use as substrate of the heating elements. It is widely used in microelectronics and in hybrid integrated circuits in particular. This material was prefered because of its advantageous properties, such as:

- It does not contain volatile components and thermal dissociation of oxides in the ceramics composition occurs at temperatures higher than those necessary for processing technology.
- It has high volume resistance which practicaly remains constant in the process of wear and is slightly affected by temperature. It has high electric resistance and perfect insulating properties.
- It has high heat conductivity, much higher than that of standart insulating materials.
- It is inert to effects of various chemicals and highly resistant to humidity, fog, mist, etc.
- It has good contractability in all directions and appearance which practicaly does not change with ageing. Elements with a size of some fractions of milimeter up to some hundred milimeters can be made.
- Ceramics composition is mainly Al_2O_3, which is cheap and avaible material.

All samples were prepared on square 96% Al_2O_3 ceramic substrates with a side of 2 inch (50.8 mm) and 0.9 mm thick. Thick film inks are deposited on substrates by a screen printing process. The ink consists of four distinct groups of intermediates, which are thoroughly mixed and blended, yielding a homogeneous product – Table 1 [5](http://www2.dupont.com/MCM/en_US/techtip/basics.html, February 2014).

Table 1. Typical ingredients of a thick film ink

Functional Phase	Consists of metal powders (Pt,Pd,Ag,Au, etc.) in conductive inks, metals and/or metal oxides (RuO_2, Bi_2 Ru_2O_7, Pd, Ag) in resistors and ceramic/glass ($BaTiO_3$, glass) in dielectric temperature firing.
Binder Phase	Serves to hold the ink to the ceramic substrate, and merges with the ceramic during high temperature firing.
Vehicle	Acts as the carrier for the powders and is composed of both volatile (solvents) and non-volatile (polymers) organics. These evaporate and burn off during the early stages of drying and firing, respectively.
Modifiers	These are small amounts of proprietary additives which control behavior of the inks before and after processing.

Screen printing requires the ink viscosity to be controlled within limits determined by other rheological properties, such as the amount of inorganic powders in the ink. The printing screen is prepared by stretching stainless steel wire mesh cloth across the screen frame and attaching it, maintaining high tension of the mesh. An organic emulsion is then spread over the entire mesh, filling all open areas. The area to be screen printed is then patterned on the screen. As the squeegee moves the ink across the screen, a shearing action causes a decrease in viscosity, allowing the ink to pass through the patterned areas, onto the substrate. As the squeegee passes, the screen peels away and the ink viscosity recovers, leaving a well defined print. Dry print thickness can be varied by employing a different screen mesh – Table 2 (http://www2.dupont.com/MCM/en_US/techtip/basics.html, February 2014).

Table 2. Typical dry print thicknesses depending on the applied screen mesh

Screen mesh	Typical dry print thickness, μm
200	25
200	26
250	21
325	16

From these data, it can be seen the screen mesh is critical, when determining the desired thick film print thickness.

The essential advantages of the screen printing technology are:

- good adhesion with the ceramic substrate;
- controllable changes of the electric resistivity before and after layering;
- good corrosion resistance;
- the coefficient of thermal expansion of the resistive layer is close to that of the substrate.

The samples are produced using a technology similar to that for the production of Printed Circuit Boards with a number of special technological features.

The experimental production was realized in the Laboratory of CONIS ELCO Ltd. (former Capacitor plant, Kyustendil, Bulgaria). Two types of samples were produced, using Al_2O_3 ceramic substrates and screen printing technology of formation of the resistive and protective layers and of the contact terminals sites.

Special conductive inks with high viscosity were applied. The main features of the samples are described in Table 3.

Table 3. Main features of the samples

Type of sample	Substrate	Resistive layer	Protective layer	Contact terminal site
Type 1	96%Al_2O_3 ceramic, Rosenthal, Germany	Conductive ink 8041, 10 kOhm/sq DuPont, USA	Dielectric ink IP9025S, Heraeus, Germany	Conductive silver-based ink C1206, Heraeus, Germany
Type 2	96%Al_2O_3 ceramic, Rosenthal, Germany	Conductive ink R4005B, 100 Ohm/sq Heraeus, Germany	Dielectric ink IP9025S, Heraeus, Germany	Conductive silver-based ink C1206, Heraeus, Germany

After applying the inks the samples are dried at 120 ^{o}C and fired at 825-875 ^{o}C.

KAMMANN Screen Printing Unit K15QSL is used – Figure 1. The screen printing machine of the K15 series is designed for printing on flat materials with medium to high viscosity fluids. The entire screen frame mounting is translational and rotative adjustable. Other parameters such as squeegee angle, squeegee pressure and printing speed can be varied.

Fig. 1. General view of KAMMANN Screen Printing Unit K15QSL

The parameters of the technological process were as follows: screen mesh – 200, speed of the squeegee – 35 mm/s, thickness of the emulsion layer of the screen – 11 mm, mean firing temperature – 850 ^{o}C, time of maintaining maximal firing temperature – 10 min, paste viscosity – 105 Pa.s.

In experimenting the procedures mentioned parameters were changed many times and their effects upon the quality of the layer were studied by statistic analysis.

An entire protective layer covering entire plane of the element on the side of the resistive layer was applied on samples of heater elements by screen printing, this layer enabling operation of the heater in direct contact with conducting objects without using additional insulation.

The configuration of the samples of heater elements is shown in Figures 2 and 3.

Prototypes (samples) are developed with the following parameters: area of the heater – 2,58. 10^{-3} sq. m, maximal power for this area – 60 W, maximal operating temperature – 380 ^{o}C, dielectric strength - 1500 VAC. Power supply may be of direct or alternating current of up to 250 V.

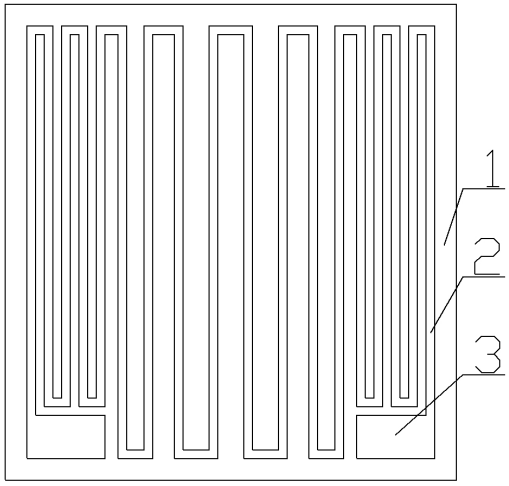

Fig. 2. Configuration of the resistive layer of the samples, wherein: 1 – ceramic substrate, 2 – resistive layer, 3 – contact terminal sites

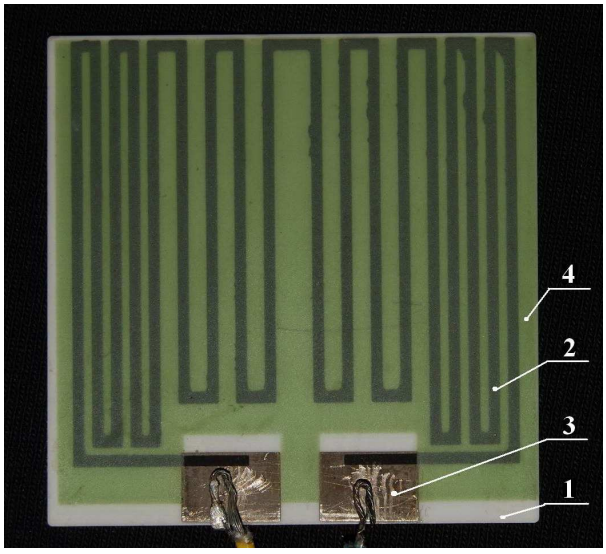

Fig. 3. General view (photo) of a heater element sample, wherein: 1 – ceramic substrate, 2 – resistive layer, 3 – contact terminal sites, 4 – protective layer

3. LEAKAGE CURRENT MEASUREMENT

A micro ammeter specially designed for measuring leakage currents is used. A copper foil of a specific size is placed on the heater, and the current flowing from it to ground is measured. Two types of measurements are performed: measurement of the leakage current, flowing from the heater's ceramic substrate and measurement of the leakage current flowing from the protective printed layer. The leakage currents are measured in regime of increasing the operating temperature of the heater. The results of the measurements are shown in Figures 4 and 5.

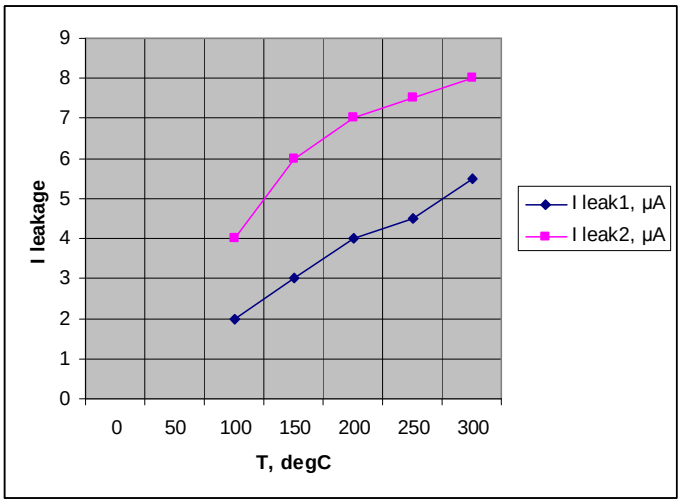

Fig. 4. Leakage current, flowing from the heater's ceramic substrate to ground, wherein: I_{leak1} – leakage current of sample type 1, I_{leak2} – leakage current of sample type 2

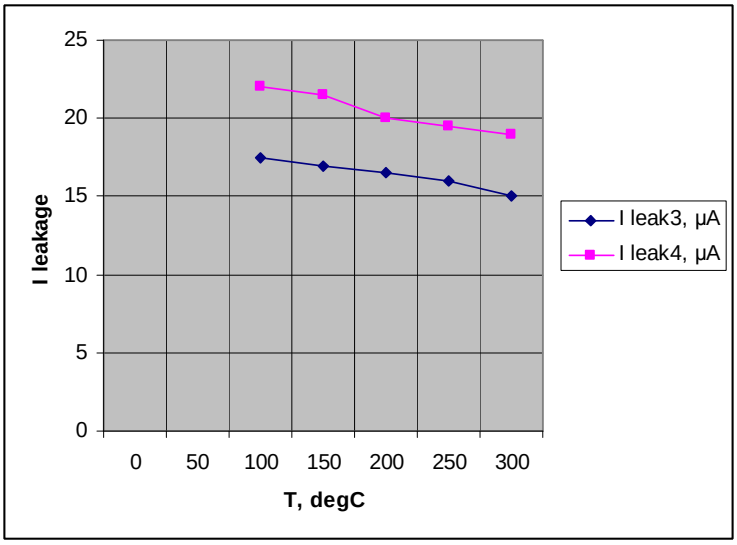

Fig. 5. Leakage current flowing from the protective printed layer to ground, wherein: I_{leak3} – leakage current of sample type 1, I_{leak4} – leakage current of sample type 2

The safe levels of the leakage currents have been determined by the IEC 950 safety standard. Most countries around the world have adopted this standard. The limits are defined in Table 4.

Table 4. IEC 950 Safety standard levels of leakage currents.

Equipment type	Max. leakage current
Double insulated all	0.25 mA
Grounded hand held	0.75 mA
Movable (other than hand-held)	3.5 mA
Stationary (permanently connected)	3.5 mA

The analysis of the experimental results led to the following conclusions:

- The leakage current in all experiments is about 10 times lower than the limit values of the standard.
- The leakage current through the protective insulating layer is about 2 times larger than the leakage current through the substrate. This is due to their different thicknesses. The thickness of the substrate is 0.9. 10^{-3} m, while insulating protective layer is 15. 10^{-6} m.

4. METHODS AND APPARATUS FOR CONDUCTING THE TESTS OF CORROSION RESISTANCE

Standard tests for resistance to the impact of sea mist of the samples of heating elements were performed.

The tests were conducted in the Laboratory for material analysis and testing and calibration of measuring facilities (LMTC) of the “Acad. A. Balevski” Institute of Metal Science of the Bulgarian Academy of Sciences.

Testing was made in an aerosol chamber Aerozol-Korrosionsprufkammera Type 1000 – Switzerland - Figure 6, in accordance with standards BS EN ISO 7384:1996 and BS EN ISO 9227:2007, in a medium of neutral salt mist. The experiments were performed with the following parameters of the procedure:

- chamber temperature T = 35.0℃;
- composition of the solution of salts: sodium chloride NaCl - 27g / l; magnesium chloride $MgCl_2$ - 6 g / l; calcium chloride $CaCl_2$ - 1 g / l; potassium chloride KCl - 1 g / l;
- duration of the injection of the solution in the chamber - 15 minutes per hour;
- total duration of the test – 48 hours.

Ten samples of heating elements were tested and before and after the experiment the active resistance of their resistive layer was measured. The maximum change recorded from the initial resistance is 1.23% which is considered acceptable.

5. CONCLUSIONS

The proposed process for obtaining protected printed thick film heating elements is considerably simpler than the classical technology applied for the production of tubular heaters for ships.

The proposed heating elements are suitable for use in direct contact with conductive objects without the use of additional insulation details due to the low values of leakage current through the ceramic substrate and the protective layer.

Fig. 6. General view of aerosol chamber Aerozol-Korrosionsprufkammera Type 1000

The proposed heating elements are made by additive technology by eliminating the mechanical contact of two or more bodies forming the heater which may lead worsening the thermal contact and decreasing the reliability of the heaters.

There is no technological barrier to applying the protective layer after attaching the contact terminals, which strengthens mechanically the terminals and seal them.

The proposed heating elements have a very good resistance to high humidity environments and environments containing salts (sea mist). Therefore, they can find application in navigating heating appliances working in indoor ship areas.

The heater elements on ceramic substrates are considered promising and we have been working on their further modifications. The resulting samples of heating elements are registered as a patent for utility model at the Patent Office of Bulgaria - Patent № BG-1523/15.07.2011.

REFERENCES

[1]. http://www.nauticexpo.com/boat-manufacturer/immersion-heater-ships-21998.html
[2]. http://www.indeeco.com/Indeeco_C21_1_reduced.pdf
[3]. http://www.ehow.com/list_7699984_disadvantages-tubular-heating-elements.html
[4]. http://www.tempco.com/Catalog/Section%209-pdf/Thick%20Film.pdf
[5]. http://www2.dupont.com/MCM/en_US/techtip/basics.html

NEW TRENDS IN THE CONTENT OF THE BULGARIAN NAUTICAL NAVIGATION CHARTS

DACHEV YURIY

Nikola Vaptsarov Naval Academy - Varna, Bulgaria

International standard for nautical navigation charts consists in international nautical navigation charts and their symbols. This charts are published by the United Kingdom Hydrographic Office. From several years we have seen new trends in worldwide view for preparation of the nautical navigation charts. Hydrographic Offices of many maritime countries, including Bulgaria, began to make a significant changes in the nature and the content of their modern nautical navigation charts. The most important changes are observed in the symbols, in the used colors, in the duplication of all texts on local and English languages, in standardization of the characteristics of navigational aids, in the ground of the seabed, in the sources of information, etc. The major advantage of all these changes is that the nautical navigation charts of these countries will become competitive to the international charts issued by the United Kingdom Hydrographic Office. The report examines the Bulgarian nautical navigation charts issued until now and trends in their content in accordance with international standards in this field and increases their competitiveness in the market for this product.

***Keywords**:* nautical navigation chart, hydrographic service

1. INTERNATIONAL NAUTICAL NAVIGATION CHARTS

Bulgarian nautical charts are compiled and published by the Hydrographic Office of the Navy, which was established in 1883. First Bulgarian hydrographic survey of Bourgas Bay was performed in 1896. In 1904 was created the first Bulgarian nautical chart, applying for the Bulgarian section of the river Danube. First Bulgarian nautical plan of Varna Bay was published in 1909. Nowadays the Hydrographic Service creates nautical navigation charts and plans for the Bulgarian Black Sea coast.

International standards in this field are international nautical navigation charts issued by the Hydrographic Office of the British Admiralty. From the first British Admiralty chart, put up for sale in 1823, the British nautical navigation charts for the world's ocean in 2013 exceeds 4000 (Belchev and Nyagolova, 1997). From these navigation charts more then 640 are international. Admiralty international nautical navigation charts began to be published after 1998, when the handbook CHART 5011 "Symbols and Abbreviations used on Admiralty Charts", containing symbols (legend marks) and the abbreviation used in the english nautical charts was issued for the first time with the abbreviation INT. This symbols and abbreviations are practically declared as international. Due to the good cooperation between the British Admiralty, the International Hydrographic Organization (IHO) and the International Maritime Organization (IMO), the symbols and abbreviations are in full compliance with all requirements, concenirng content and layout of modern nautical navigation charts. Fifth edition of CHART 5011 INT was published in 2011 (NP 5011 INT, 2013). In 2012 the

publication is divided on two books – NP 5011 “Symbols and Abbreviations Used on Admiralty Paper Charts” and NP 5012 “Admiralty Guide to ENC Symbols used in ECDIS”.

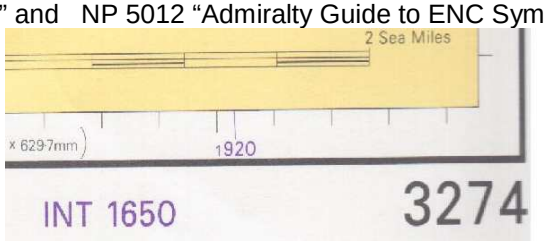

Fig. 1. International and Admiralty number of international nautical navigation charts

Admiralty international nautical navigation charts contains not only Admiralty number, but also international number. This is shown in Figure 1, where the Admiralty number of the international chart is 3274, and international number is INT 1650.

Moreover, the title of international nautical navigation charts except the seal of the Hydrographic office of the British Admiralty, contains also the seal of IHO. (Fig. 2) The seals are limited by the inscription "INTERNATIONAL CHART SERIES".

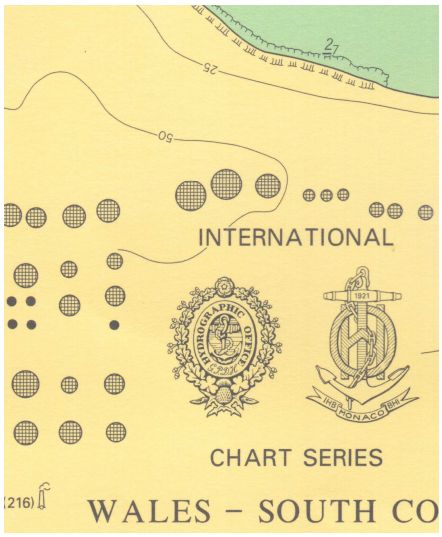

Fig. 2. The seals in the International nautical navigation chart

2. STATE OF THE BULGARIAN NAUTICAL NAVIGATION CHARTS

Bulgarian nautical navigation charts in comparison with charts from the Admiralty international series differ in many indicators - in texts, in symbols, in colors, in their overall layout and etc.

From a practical point of view the following significant disadvantages of the Bulgarian nautical navigation charts can be mentioned:

- The inscriptions and texts are not duplicated in English, which makes them unusable by foreign users;

- The symbols used for objects displaying differ considerably from symbols in the handbook CHART 5011 INT, which are without significant changes from the 70s of the last century (HO Navy, 2011) ;

- The information concerning corrections to the latitude and longitude determined by receiver GPS is missing. This corrections arise due to the difference between the ellipsoid of Krasovsky 1940, which is used as a model of the Earth in working out of Bulgarian charts, and ellipsoid WGS 84, used by the global satellite navigation system "NAVSTAR GPS". This information was announced a few years ago in Notice to Mariners and had to be additionaly inserted on the charts as a corrections for the latitudes and longitudes;

- There are no compass roses with magnetic variation (declination) data for various sea water regions of the chart and only the text in the title of the chart gives summarized information for the whole sea area. Although the difference in magnetic variations for the whole Bulgarian Black Sea coast is about 5-6 minutes, it is properly the same to be shown on the various compass roses;

- The sources for geodetic, cartographic and hydrographic data used to compose the charts are missing;

- The charts numbering is unusual and difficult to remember;

- The ellipsoid, used for composing the charts is not specified;

- The cartographic projection used for chart drawing is not mentioned;

- The abbreviations for the ground of the seabed and the characteristics of lights and buoys are given in Bulgarian letters, and a comparative table (legend) for alignment with the international abbreviations is missing;

- There is no information for the region of the IALA buoyage system and etc.

3. NEW TRENDS IN THE ISSUANCE OF THE BULGARIAN NAUTICAL NAVIGATION CHARTS

From 2011 the Hydrographic Office of Navy began issuing nautical navigation charts and plans very similar to the international. When looking at the new navigation plan of the Bourgas Bay 010.50 in scale 1:10 000, many positive changes can be seen, which make them actual and competitive on the market of these products (HO Navy, 2011).

One of the most important achievements of the new plan is, that it is prepared under WGS 84 ellipsoid, which automatically eliminate the need for corrections to the GPS-coordinates and they can be directly ploted on the plan. (Fig. 3) Another important accomplishment of the new plan is that all text information is duplicated in Bulgarian and English. (Fig. 4)

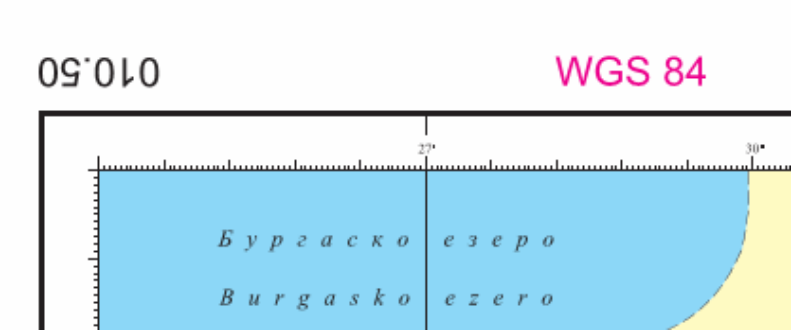

Fig. 3. Part of the new nautical navigation plan 010.50 of the Bay of Bourgas

Moreover, in the title of the plan are listed the elevation system of the points from the shore and the region of the IALA buoyage system. (Fig. 4) The comparative table, which gives symbols of Bulgarian international abbreviations for colors and characteristics of the headlights and ground of the bottom is situated over the shore. The colors of the plan are changed in accordance with international charts.

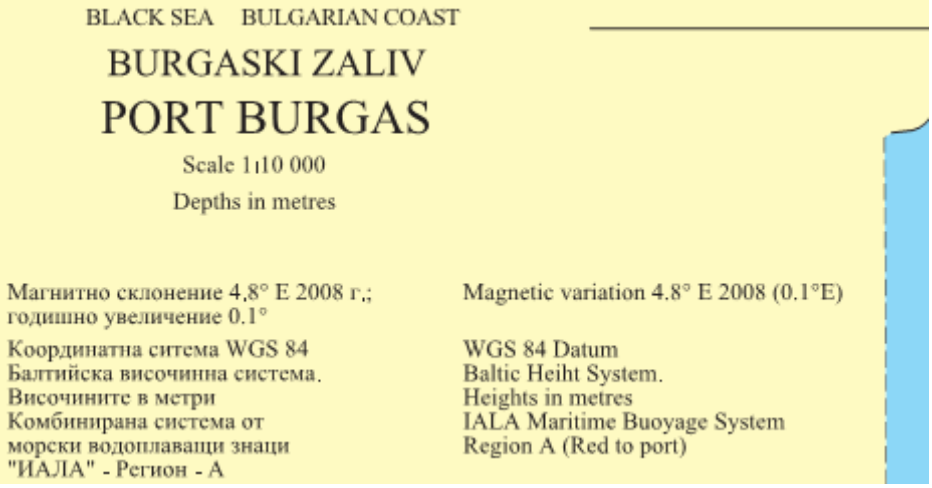

Fig. 4. Text in the title of the new nautical navigation plan 010.50 of the Bay of Bourgas

New nautical navigation plan is a significant step towards bringing the Bulgarian nautical navigation charts and plans in accordance with the international. Few important things need to be done which will change the whole look of our charts and plans – the symbols had to be changed, the compass roses for magnetic variation had to be preapared, the alteration to international abbreviation for the characteristics of the headlights and ground of the bottom had to be done. The Bulgarian nautical navigation charts and plans will become much more competitive in the market of these products, as soon as the other things are done.

4. CONCLUSIONS

Despite the massive entering of electronic nautical charts in modern maritime navigation, the importance of the paper nautical navigation charts will not be reduced. Regardless of the ongoing modernization of the technical aids of navigation, the paper charts will always play a part in improving the safety of navigation. The investments in modernization and standardization of the modern paper nautical navigation charts is not a lost cause. It is necessary and profitable at the same time.

REFERENCES

[1]. Belchev M., H. Nyagolova - ***English international and Admiralty charts***, Steno, Varna, 1997
[2]. HO Navy -***Nautical plan 010.50 of the Bay of Bourgas***, HO Navy, Varna, 2011
[3]. HO Navy - ***Symbols of Bulgarian charts***, HO Navy, Varna, 1978
[4]. NP 5011 INT **(*CHART 5011 INT), "Symbols and Abbreviations used on Admiralty Paper Charts"***, The United Kingdom Hydrographic Office, Taunton, 2013

QUANTUM DOTS INTERACTION WITH PROKARYOTES INVOLVED IN THE MARINE BIOREMEDIATION PROCESS

[1]GHITA SIMONA, [2]SARCHIZIAN IRIS

[1]Constanta Maritime University, [2]County School Inspectorate of Constanta, Mihai Eminescu no. 11, Romania

Semiconductor nanocrystals (quantum dots QDs) are known to show desirable optical characteristics like photostability, fluorescence properties, broad absorption spectra and size-dependent narrow emission spectra, leading to major advances in medical diagnostics, targeted therapeutics, microbiology, molecular and cell biology. In this paper we present our results concerning the interaction of CdSe/ZnS core-shell quantum dots (490 nm; 520 nm; 560 nm and 600 nm) with long chain amine capping agent with hydrocarbon-oxidizing bacteria. The biological samples used are natural populations of cyanobacteria and heterotrophic bacteria from the Black Sea. Quantum dots that emit at 520 nm and 600 nm allow the visualization of the microorganisms, but the experimental values obtained are close to the number of dead cells (PI positive) and not the total number of cells (DAPI), suggesting that QD label almost exclusively dead cells.

***Keywords**:* semiconductors nanocrystals, microorganism, microcosms.

1. INTRODUCTION

Maritime transport processes intensification inevitably attracts hydrocarbons water pollution and for this reason it should be taken into account the respect for international norms regarding the marine pollution as well as the intervention ways (Swannell et al., 1996; Gouda et al., 2008; Acomi and Acomi, 2013). We must start from the clearest possible premises of understanding the nature occurring processes (Ghiță, 2009). Microorganism's role in oil consumption is very important, precisely because of their ability to adapt to extreme conditions (e.g. little sunlight, small amount of nitrogen available, and pollutants presence, so on). These microorganisms play an important role in decomposition and mineralization of organic matter, thus contributing to the restoration of aquatic ecosystems polluted with oil (Röling et al., 2002). The organisms can be characterised phenotypically or physiologically and their roles in the environment can be deduced. Using digital image analysis algorithms obtained by combining mathematical methods from CellC and ImageJ software made it possible, to precisely identify in a relatively short time the number of cells analyzed in microorganisms from digital images taken in epifluorescent microscope field.

The aim of this paper is to evaluate the physiological status of heterotrophic and autotrophic bacteria in microcosms supplemented with gasoline and ammonium nitrate. These microcosms are experimental model systems for natural marine environments. In this paper we have studied also the interaction between nanoparticles quantum (CdSe/ZnS) and

hydrocarbon-tolerant bacteria, as well as highlighting the fluorescence of microorganisms marked with quantum dots.

2. MATERIALS AND METHODS

We collected water samples from the Black Sea (1m depth) which was used for the microcosm's setup done in Polyethylene transparent bottles. Taking into account the advantages of microcosms (Gregori et al., 2003; Molina-Barahona et al., 2004) we used this opportunity as previously (Ardelean et al., 2009). In our experiments, the microcosms in volume 2 L of natural sea water were kept at ambient temperature and natural illumination for two months (from April 15 to June 20, 2013). Five following types of microcosms are: natural sample- control (M3); control supplemented with petroleum hydrocarbons (gasoline-1% v/w) and nutrients (ammonium nitrate- 0.005% w/w; ammonium phosphate 0.005% w/w) (M1); control supplemented with petroleum hydrocarbons (gasoline-1% v/w) (M2); control supplemented with gasoline (1% v/w) and selected population - 1 mL (M4) and control supplemented with gasoline (1% v/w), nutrients (ammonium nitrate 0.005% w/w; ammonium phosphate 0.005% w/w) and selected population – 1 mL (M5). Selective cultivation was made as previously shown (Ghiță, 2013). Sampling was done sequentially at 1, 7, 14, 21, 39 and 55 days from the start of the experiment and fixed with buffered formaline (2% final concentration) and kept at 4^{o}C in darkness without any added fluorochromes.

1. Total cell and dead cell counting

Total cell count was done using DAPI (5 µg/mL dye final concentrations) with the time staining by 5 minutes. Dead cells were counted using propidium iodide (PI) – 2 µg/mL dye final concentrations, with the same time staining. Samples were filtered on black Millipore 0.22 µm pore size filters, for quantification of bacterial cells. Filters were subsequently inspected under an epifluorescence microscope (Fl5 and N-400FL type, lamp Hg 100 W, blue filter 450-480 nm). The disruption of planktonic cell aggregates for cell enumeration was done as previously shown (Ardelean et al., 2009). Cell enumeration was done automatically using the CellC software (http://www.cs.tut.fi/sgn/csb/cellc/) and a calibrated square eye piece (Surface 0.01mm^2). In addition, we used Cell Profiller to perform our experiments - counting cells, measuring the intensity of fluorescently labelled cyanobacteria filaments with QD.

2. View heterotrophic and phototrophic bacteria using fluorescent quantum dots

The biological samples suspension (intact cells or bleached cells - commercial bleaching agent) were filtered through Millipore filters (0.22 micrometers) or used directly on microscopic slides. Contact natural samples with bleaching agents were about 1-2 minutes. The microphotographs taken with a Panasonic digital camera (DMC-FZ28; 10 megapixels; 18 x optical zoom) were used for automated image analysis and heterotrophic cells enumerations (Selinummi et al., 2005). Quantum dots produced by Evident Technologies with the following specification of colour, emission, form, crystal diameter, molar extinction coefficient, molecular weight, quantum yield, 1st excitant peak, emission peak tolerance, as previously shown (Ardelean et al., 2011).

3. RESULTS AND DISCUSSION

In experimental microcosms we viewed the gasoline tolerant-oxidizing phototrophic bacteria and heterotrophic bacteria at the epifluorescence microscope to make a clear distinction between the cells stained with DAPI (for the total number) and dead cells fraction (PI staining) – Figure 1.

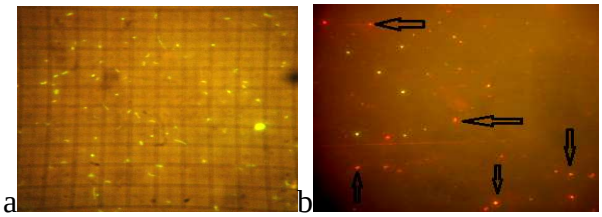

Fig. 1. (a) DAPI staining; (b) PI staining (arrows indicate the presence of PI (+) cells)

Quantum dots that emit at 520 nm and 600 nm allow the visualization of the heterotrophic microorganisms from five microcosms, but the experimental values obtained are close to the number of dead cells (PI positive) and not the total number of cells (DAPI), suggesting that QD label almost exclusively dead cells (Figure 2).

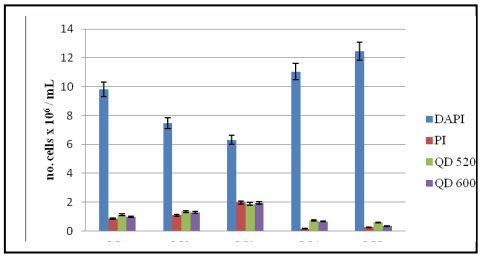

Fig. 2. Quantification of heterotrophic bacteria using different fluorochromes in five experimental samples (n=20)

Fluorescent dots 520 nm and 600 nm were chosen, as allowed best viewing of natural prokaryotic, as can be seen in Figure 3. Advantages of using quantum dots are the following: they have a very high yield of fluorescence than classical fluorochromes; quantum dots stability under normal conditions is indefinitely; the absorption and emission spectra is very narrow, which allows a better selectivity of the analysis cell. Microcosm's seawater is an oligotrophic environment (Ghiță, 2007) and at the beginning of the experiment we had a positive response to nitrogen supplementation in M1 and M5. After environment nitrogen depletion the bacteria fractions have been reduced significant (Cohen, 2002). In case of nitrogen and carbon "starvation", literature mentions that carbon as the limiting factor compared with other nutrients (Holmquist & Kjelleberg, 1993). Also, in M2 and M4 was selected a microbiota composed of microorganisms able to tolerate and / or oxidize gasoline hydrocarbons. This fact is also reflected by difference PI (+) cell fraction of the five microcosms (M1: 0.85 $x10^6$ cells mL^{-1} ± 0.5 SD; M2: 1.09 $x10^6$ cells mL^{-1} ± 0.26 SD; M3: 1.97 $x10^6$ cells mL^{-1} ± 0.66 SD; M4: 0.16 $x10^6$ cells mL^{-1} ± 0.07 SD; M5: 0.26 $x10^6$ cells mL^{-1} ± 0.34 SD), cumulated with data generated by quantum dots. There are small differences in total counts obtained by the use if PI and QD, the higher count obtained with 520 nm QD (an average of 16%), being due to its higher fluorescent yield.

The biodegradation of different individual components from gasoline have been studied from the point of view of both aerobic and anaerobic processes (data not shown). The experimental difficulties are mainly given by aerobic conditions to prevent volatilization of low hydrocarbon fractions. The differences in substrate use (experimental microcosms 2, 4 and 5) can appear due to factors which may restrict the utilization of some strains or species, which have various sensitivities towards biotoxic effect of certain hydrocarbons. Gasoline

hydrocarbons are the growth substrates for microorganisms due the fact it provides energy and carbon source (Prince et al., 2008).

Heterotrophic hydrocarbon-tolerant bacteria and cyanobacteria visualized with QD

In our natural samples we tested four types of quantum dots emitting from green to red, wanting to put the record heterotrophic bacteria, thereby the possibility of using fluorescent dots for quantification. For heterotrophic bacteria, the specific dots fluorescence was each dot, ranging from green to deep red (490-600 nm).

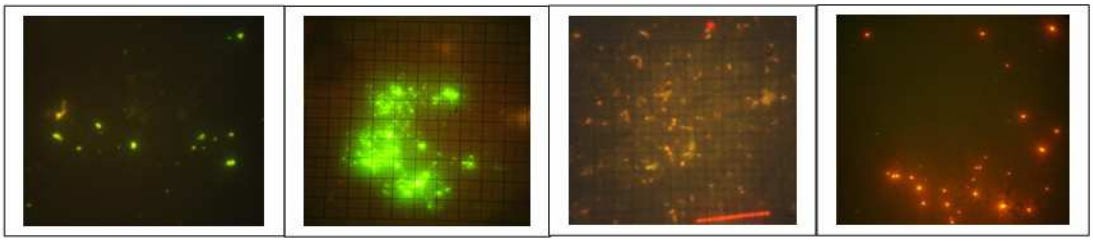

(a) (b) (c) (d)

Fig.3. Heterotrophic hydrocarbon-tolerant bacteria visualized with QD: (a) QD 490 nm; (b) 520 nm; (c) 560 nm; (d) 600 nm

Before being subjected to dots fluorescent staining technique, natural samples have been discoloured by bleach, observing that if quantum dot changes fluorescence colour. Even after the killing gasoline-tolerant/oxidant heterotrophic populations by applying chemical agents (chlorine) and physical agents (heat treatment), specific fluorescence of quantum dot has not changed. Difference in fluorescence intensity is observed for 520 nm and 600 nm QD (which shows increased fluorescence intensity compared with 490 nm and 560 nm QD). In microcosm supplemented only carbon source (M2 and M4) we have noticed the presence of some filamentous cyanobacteria (Ghiță and Ardelean, 2010). Musat and collaborators (2006) have reported the existence of molecular nitrogen fixation process independent of light conditions (in marine sediments contaminated by hydrocarbons), without indicating systematic group which fix nitrogen molecular. These filamentous cyanobacteria have been measured automatically with CellC program, by gradually adding fluorescent dot. In the case cyanobacteria staining with QD, fluorescence colour is almost unchanged (it remains in the red-orange spectrum) (Figure 4).

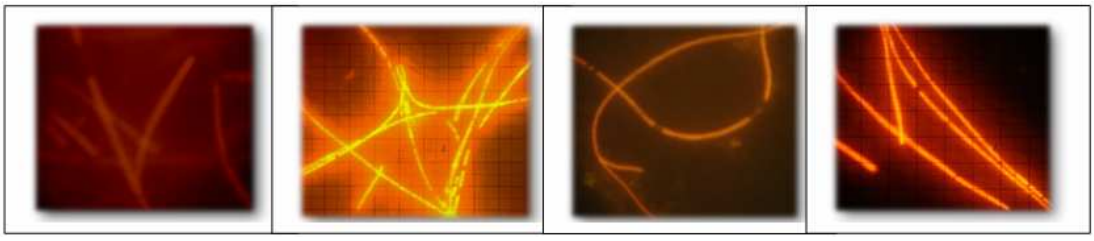

(a) (b) (c) (d)

Fig. 4. Living cyanobacteria from marine microcosm's samples visualized with QD: (a) QD 490 nm; (b) 520 nm; (c) 560 nm; (d) 600 nm

The difference is due to the absence of fluorescent emission of chlorophyll *a* in the case of preparations which chlorophyll was oxidized. A good example is the time evolution observation of the microcosm's interaction with the quantum dots (QD 520 nm) evidenced by the change of the bacteria cell fluorescence colour and also we have take in consideration

the preliminary investigation of cytotoxicity prokaryotes due to interaction between quantum dots (CdSe/ZnS) and hydrocarbon-tolerant microcosms bacteria. Digital images processing was performed with CellC program and image capture was done using epifluorescence microscopy. Further we have studied the interaction between cyanobacteria filament and QD 520 nm, and we have noticed that after a first few seconds of interaction, the filament became red due to the presence of chlorophyll *a*, but after one minute sheath of cell membrane was damaged, a phenomenon attributed to the toxic effect of QD (Ardelean et al., 2011). Through digital image analysis in various colour channels (red, green, blue), we can assume that these nanoparticles may be accumulated at the surface of microorganisms, there is practically a physical process of interaction between prokaryotic cell and QD (Zeder et al., 2010).

Studying the fluorescence images from the microcosm's marine sample in which quantum dots were added, we have observed changes in the fluorescence colour from the pale orange colour to deep green in less than four minutes after QD addition. After adding multiple semiconductor nanocrystals 520 nm quantities the colour modification was observed using green channel interaction, because the fluorescence intensity of the green fluorescent quantum dots is slightly higher than on the red channel. This observation had been possible after backgroud substraction of digital image using Image J software (Figure 5), (http://rsbweb.nih.gov/ij/).

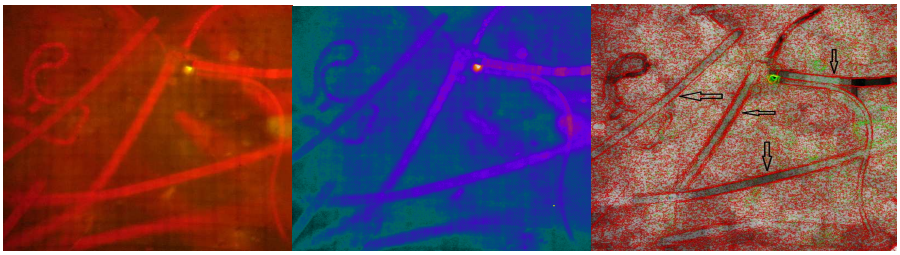

(a) (b) (c)

Fig. 5. Fluorescence cyanobacteria filaments from gasoline supplemented microcosms: (a) natural fluorescence of cyanobacteria; (b) image obtain after extraction stages image substrate at 1-2 seconds and (c) 1 minute

This modern method makes possible the detection of quantum dot - cyanobacteria filament interaction, observing the migration of QD toward filaments direction and remains attached to their sheath (registration through intense points from Figure 5c).

As a conclusion, we have noticed the existence of a difference between autotrophic and heterotrophic prokaryotes. QD-cell interaction at heterotrophic bacteria is followed by differential staining, specific for each fluorescent dot. Instead, at the phototrophic bacteria, this chlorophyll lead to an overlay colour (for example, red-chlorophyll *a* and green-QD). In conclusion, the green channel intensity increases with increasing time of exposure to quantum dots (from 15 pixels at 96 pixels in four minutes).

4. CONCLUSIONS

These results are very important for the bioaugmentation studies that involve biostimulation methods of microbiota in microcosms (as experimental model systems for natural marine environments) contaminated with hydrocarbons. Multidisciplinary character of quantum dots aims to understanding the interaction mechanisms of semiconductor nanocrystals with prokaryotes, by using automated analysis programs of digital images obtained with the epifluorescence microscope.

ACKNOWLEDGEMENTS

Thanks are due to dr. tech. Jyrky Selinummi (Finland) for kind support for digital image analysis and to Dr. Ileana Apostol (Romania) for kindly providing the quantum dots.

REFERENCES

[1]. Acomi N., Acomi O.C. - ***Computer based program for fitting cargo area foam fixed fire-fighting equipment on chemical tankers***, Developments in Maritime Transportation and Exploitation of Sea Resources: IMAM, ISBN 978-1-138-00124-4, pp.705-709*,* 2013
[2]. Ardelean I.I., Ghiță S., Sarchizian I. - ***Epifluorescent method for quantification of planktonic marine prokaryotes***, Proceedings of the 2nd International Symposium "New Research in Biotechnology"*,* serie F, pp. 288-296, 2009
[3]. Ardelean I.I., Sarchizian I., Manea M., Damian V., Apostol I., Cirnu M., Armaselu A., Iordache I., Apostol D. - ***CdSe/ZnS quantum dots cytotoxicity against phototrophic and heterotrophic bacteria,*** Nanocon, 3, pp. 608-616, 2011
[4]. Cohen Y. - ***Bioremediation of oil by marine microbial mats***, Int Microbiol., 5, pp. 189–193, 2002
[5]. Ghiță S. - ***Ecology Course***, Ed. Nautica, (Chapter 2), 2007
[6]. Ghiță S. - ***Biodiversity***, Ed. Nautica, (Chapter 4), 2009
[7].Ghiță S., Ardelean I.I. - ***Marine bacterioplankton density dynamics in microcosms supplemented with gasoline***, Rom. J. Biol- Plant Biol., 55, No 1, pp. 55-61, 2010
[8]. Ghiță S. - ***Biochemical oxygen demand and physiological state of bacteria in sea water microcosms supplemented with gasoline***, 1st Global Conference on Environmental Studies: CENVISU, 1, pp. 194-200, 2013
[9]. Gouda M.K., Omar S. H., Eldin H.M.N., Chekroud Z.A. - ***Bioremediation of kerosene II: a case study in contaminated clay (Laboratory and field: scale microcosms)***, World J Microbiol Biotechnol*,* 24, pp. 1451–1460, 2008
[10]. Gregori G., Denis M., Lefevre D., Romano J.C. - ***Viability of heterotrophic bacteria in the Bay of Marseille***, C. R. Biol*.*, 326, pp. 739-750, 2003
[11]. Holmquist L., Kjelleberg S. - ***Changes in viabilitz, respiratory activity and morphology of marine Vibrio sp. strain S14 during starvation of individual nutrients and subsequent recovery***, FEMS Microbiol. Ecol*.,* 12, pp. 215-224, 1993
[12]. Molina-Barahona L., Rodriguez-Vazquez R., Hernandez- Velasco M., Vega-Jarquin C., Zapata-Perez O., Mendoza- Cantu A., Albores A. - ***Diesel removal from contaminated soils by biostimulation and supplementation with crop residues***, Appl Soil Ecol, 27, pp. 165–175, 2004
[13]. Musat F., Harder J., Widdel F. - ***Study of nitrogen fixation in microbial communities of oil-contaminated marine sediment microcosms***, Environmental Microbiology, 8, pp. 1834–1843, 2006
[14]. Prince R., Parkerton T.F., Lee C. - ***The primary aerobic biodegradation of gasoline hydrocarbons***, Chemosphere*,* 71, pp. 1446-1451, 2008
[15]. Röling W.F.M., Milner M.G., Jones D.M., Lee K., Daniel F., Swannell R.J.P., Head I.M. - ***Robust Hydrocarbon Degradation and Dynamics of Bacterial Communities during Nutrient-Enhanced Oil Spill Bioremediation***, Applied and Environmental Microbiology, 68, pp. 5537–5548, 2002
[16]. Selinummi J., Seppälä J., Yli-Harja O., Puhakka J.A. - ***Software for quantification of labeled bacteria from digital microscope images by automated image analysis***, BioTechniques, 39, pp. 859–863, 2005
[17]. Swannell R.P.J., Lee K., McDonagh M. - ***Field Evaluations of Marine Oil Spill Bioremediation***, Microbiological Reviews, 60, pp. 342–365, 1996
[18]. Zeder M., Van den Wyngaert S., K□ster O., Kathrin M., Felder K.M., Jakob Pernthaler J. - ***Automated Quantification and Sizing of Unbranched Filamentous Cyanobacteria by Model-Based Object-Oriented Image Analysis***, Applied and Environmental Microbiology, 76, pp. 1615–1622, 2010
[19]. http://www.cs.tut.fi/sgn/csb/cellc/
[20]. http://rsbweb.nih.gov/ij/

AUTOMATED AND MECHANICAL EQUIPMENT FOR COLLECTING OF METEOROLOGICAL INFORMATION ON BOARD OF THE SHIP

GRANCHAROV IVAYLO

"Nikola Vaptsarov" Naval Academy, Varna, Bulgaria

The need for reliable, accurate and comprehensive information about the weather conditions is essential for the safety of shipping. This paper discusses the various types of equipment for obtaining information about meteorological parameters on board of the vessels, their advantages and disadvantages. It emphasis the need for automation of the process to assess the weather situation in a view to save valuable time in the busiest shipping today. Officer of the Watch (OOW) should use all equipment available on board to make meteorological observations. The systems Navtex and Inmarsat-C serve to transmit MSI to ships. Constantly measuring the meteorological parameters the mariners can assess the reliability of weather forecasts prepared by coastal meteorological centers. Considering that OOW have very limited time for measuring the weather parameters, the introduction of the weather stations on board of the vessels is a key innovative technology for the safety of navigation and gives clear and precise meteorological information.

***Keywords**:* meteorology, metarea, Navtex, Inmarsat-C, safety

1. INTRODUCTION

Long time ago mariners received weather information only by Long wave radios. Nowadays meteorological forecast can be received by many different type of equipment such as VHF, MF and HF radios, Navtex, Inmarsat, Internet, Telephone, Meteofax and others. Earlier this information were compared on site with observations made by handheld anemometers, barometers and visual observations, but now most modern equipment such as computer-based stationary anemometers and marine automatic weather stations are available.

2. AUTOMATED SYSTEMS FOR METEOROLOGICAL INFORMATION, WHICH MEETS IMO REQUREMENTS UNDER GMDSS

2.1. Navtex

NAVTEX is an acronym for NAVigational TelEX. The system was used for the first time by US Coast Guard in 1983. Under the SOLAS convention it is mandatory for vessels over 300 GRT to carry on board Navtex receivers. Maritime Safety Information (MSI) is normally received by vessels at least 250 nautical miles offshore. Due to the fact that the signal is passing mostly over the open sea waters sometimes the signal can be received 400 nautical miles offshore and even more. Navtex operate in medium frequency range. Medium

frequency waves are following the Earth curves. They disseminate at a greater distance during nighttime (maximum around midnight) and winter periods, and at a lesser distance during daytime and summer periods. The innermost D layer of the ionosphere absorbs the energy of this waves and cause to their attenuation. The system operates three different frequencies 518 kHz, 490 KHz and 4209,5 kHz(IMO, 2012). Receiver can operate simultaneously on two frequencies. As a primary frequency is used 518 kHz, which is for international broadcasting. As a secondary frequency the receiver can operate one of the other two frequencies – 490 kHz is for local transmission or 4209,5 kHz which can be used in tropical areas. The latest models have three separate receivers in their circuit which allow simultaneous reception on all three Navtex working frequencies. For the purpose of collecting and transmitting the weather information to the certain vessels sailing in different geographical areas the world's ocean is divided into twenty one regions called Metareas / Navareas (Fig. 1) (WMO, 2009). Areas XVII-XXI are called Arctic Metareas. Countries assigned to prepare the meteorological bulletin for the different areas are identified as “Issuing services”. Countries contributing to the preparation of the bulletin are called “Preparation services”. In every Metarea can not operate more then 24 stations. These stations are combined in 4 groups by 6 stations each. This means that every station is allowed to transmit 10 minutes information every 4 hours. More frequent transmissions are available in the regions with less then 24 stations. Each station and type of the messages

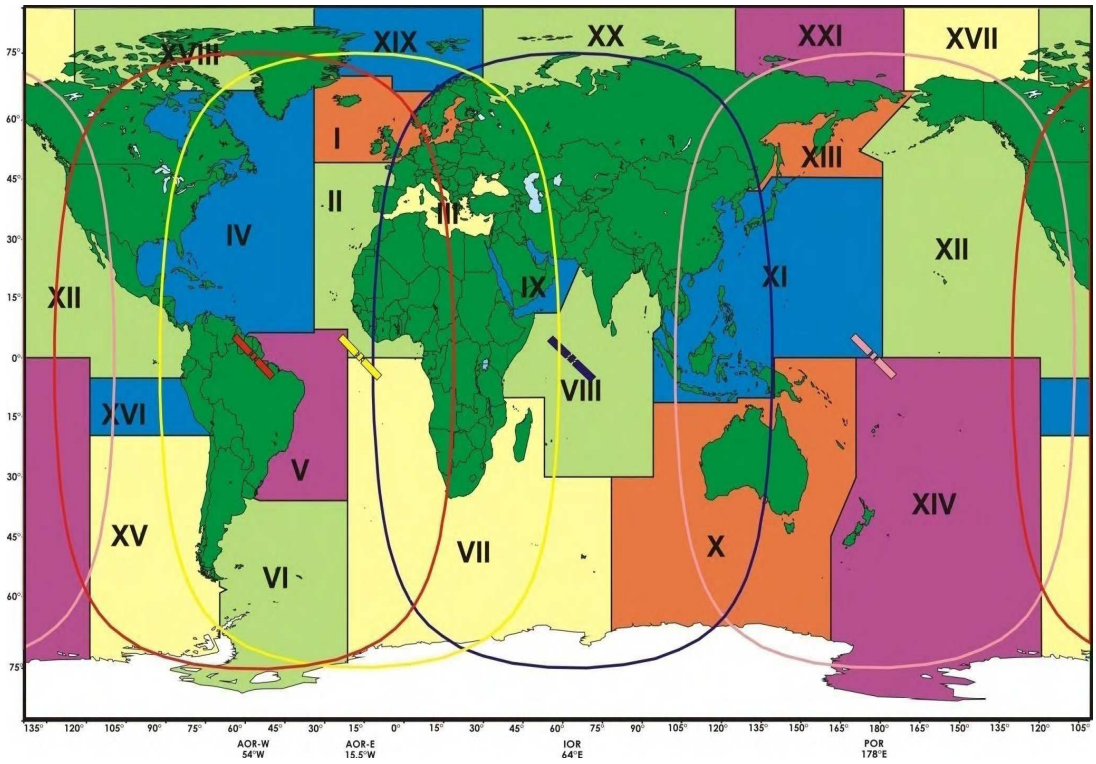

Fig.1. Metareas / Navareas

has assigned a letter from the alphabet. For meteorological information the letters are: B - meteorological warnings and E – meteorological forecast. The mariners can manually select the desired station and the information needed from the panel (Fig. 2). This adjustment is

extremely important because otherwise the OOW is overwhelmed with great amount of unnecessary information.

2.2. Inmarsat-C

Inmarsat-C maritime mobile satellite system can transmit Enhanced Group Call (EGC) messages through the service called SafetyNet. This messages allows the selected group of vessels to receive meteorological and other information when they are within the coverage of Inmarsat satellites. The system is using four geostationary satellites. Every satellite is named on the covered region: Atlantic Ocean Region – East (AOR-E), Indian Ocean Region (IOR), Pacific Ocean Region (POR), Atlantic Ocean Region – West (AOR-W). Under the SOLAS convention, after February the 1st 1999, every vessel sailing outside the Navtex service area must be equipped with Inmarsat-C SafetyNet receiver (IMO, 2009). The worldwide coverage of the satelites is up to 75^{0} N and S (sometimes up to 79^{0}), which includes almost all navigable waters (Fig. 1). The receiver (Fig. 3) can be adjusted to receive the meteorological information for the certain Metarea or for the group of areas. The type of the received messages can also be selected. Format of Navtex and Inmarsat-C EGC messages are shown in the Fig. 4 and Fig. 5. Inmarsat-C is using frequencies within the range 1.5-1.6 GHz. These frequencies disseminated practically without significant attenuation. The wave dissemination is affected by - fog, rain, dust and atmospheric water vapor. Data transmission is performed with a very high quality because the system uses sophisticated, powerful and soundproofed digital modulation codes.

Fig. 2. Navtex receiver

Fig. 3. Inmarsat-C receiver

```
-------  ZCZC UE09     PAGE 1  -------
270720 UTC OCT 12
MONDOLFO RADIO

WEATHER FORECAST OVER MEDITERRANEAN
AREAS ISSUED BY ROME METEOROLOGY CENTRE
AT 06/UTC OF 27/10/2012
AND VALID UP TO 18/UTC OF 27/10/2012
1. WARNINGS:
THUNDERSTORMS UNDER COURSE: OVER
LIGURIAN SEA, CORSICAN SEA,
SARDINIAN SEA AND CHANNEL, TYRRHENIAN
SEA, JONIAN SEA, ADRIATIC SEA
AND NORTH AND SOUTH BALEARI SEAS.
2. WEATHER SITUATION:
SEASONAL LOW ON LEVANTINE BASIN.
INSTABILITY AREA ON IONIAN SEA IS
WEAKENING AND MOVING
EAST/SOUTHEASTWARDS. HIGH AND FLAT
FIELD ON
WEST-CENTRAL MEDITERRANEAN SEA.
3. FORECAST TO 18/UTC OF 27/10/2012 AND
12 HOURS OUTLOOK:
NORTHERN ADRIATIC SEA:  SOUTHERLY 7
BECOMING SOUTHWESTERLY -ISOLATED
THUNDERSTORMS -MODERATE VISIBILITY
LOCALLY BAD -MODERATE SEA
/OUTLOOK: SOUTHWESTERLY 7 -ISOLATED
4. WIND AND SEA OUTLOOK OVER ITALIAN
SEAS FROM 06/UTC OF TOMORROW
NORTHERN ADRIATIC SEA: SOUTHWEST 4 SEA
5/EAST 3 SEA 4/NORTH 4 SEA
4/NORTHEAST 3 SEA 3.
```

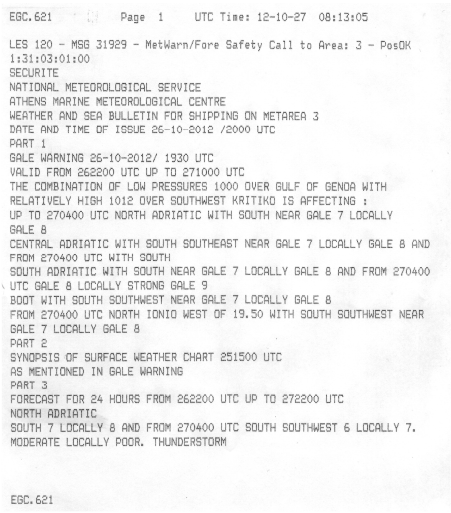

```
EGC.621      Page  1     UTC Time: 12-10-27  08:13:05

LES 120 - MSG 31929 - MetWarn/Fore Safety Call to Area: 3 - PosOK
1:31:03:01:00
SECURITE
NATIONAL METEOROLOGICAL SERVICE
ATHENS MARINE METEOROLOGICAL CENTRE
WEATHER AND SEA BULLETIN FOR SHIPPING ON METAREA 3
DATE AND TIME OF ISSUE 26-10-2012 /2000 UTC
PART 1
GALE WARNING 26-10-2012/ 1930 UTC
VALID FROM 262200 UTC UP TO 271000 UTC
THE COMBINATION OF LOW PRESSURES 1000 OVER GULF OF GENOA WITH
RELATIVELY HIGH 1012 OVER SOUTHWEST KRITIKO IS AFFECTING :
UP TO 270400 UTC NORTH ADRIATIC WITH SOUTH NEAR GALE 7 LOCALLY
GALE 8
CENTRAL ADRIATIC WITH SOUTH SOUTHEAST NEAR GALE 7 LOCALLY GALE 8 AND
FROM 270400 UTC WITH SOUTH
SOUTH ADRIATIC WITH SOUTH NEAR GALE 7 LOCALLY GALE 8 AND FROM 270400
UTC GALE 8 LOCALLY STRONG GALE 9
BOOT WITH SOUTH SOUTHWEST NEAR GALE 7 LOCALLY GALE 8
FROM 270400 UTC NORTH IONIO WEST OF 19.50 WITH SOUTH SOUTHWEST NEAR
GALE 7 LOCALLY GALE 8
PART 2
SYNOPSIS OF SURFACE WEATHER CHART 251500 UTC
AS MENTIONED IN GALE WARNING
PART 3
FORECAST FOR 24 HOURS FROM 262200 UTC UP TO 272200 UTC
NORTH ADRIATIC
SOUTH 7 LOCALLY 8 AND FROM 270400 UTC SOUTH SOUTHWEST 6 LOCALLY 7.
MODERATE LOCALLY POOR. THUNDERSTORM

EGC.621
```

Fig. 4. Navtex message ***Fig. 5. Inmarsat-C EGC message***

When the ship is sailing near the coast mariners can obtain information by both systems, while on ocean going voyages only Inmarsat-C can be use. Advantages and disadvantages of the systems are listed in Table 1.

Table 1: Advantages and disadvantages of Navtex and Inmarsat-C systems

Equipment	Advantages	Disadvantages
Navtex	- Low price; - Easy to operate; - Alows broadcasting on local language; - The system is automated, receiver can be configured.	- Can not be used in ocean going voyages (more then 400 nautical miles offshore); - The system is highly affected by atmospheric disturbance, fading or static interference; - Limited text information; (maximum of 370 words) and very strict format of the messages.
Inmarsat-C	- Can be used in almost all navigable waters in the world; - The system is lightly affected by atmospheric disturbance, fading or static interference; - The system is automated, receiver can be configured.	- Inmarsat C equipment package is much more expensive than Navtex; - Inmarsat-C antennas are subject to shadowing effects; -The equipment is more complicated than Navtex and requires more experienced operator.

3. MANUAL AND AUTOMATED EQUIPMENT ON BOARD OF THE VESSEL FOR MEASURING THE METEOROLOGICAL PARAMETERS

Most common weather instruments used in every vessel are: anemometer (Fig. 6 and Fig. 7), barometer (Fig. 8), thermometer and psychrometer (Shivarov A., 2011). Anemometer is device used for measuring the wind speed. The simplest example is hemispherical cup

type anemometer. Other type which give information not only for wind speed but for its direction also is windmill anemometer. This anemometer is based on the fact that when the wind direction is changed the axis of the equipment must follow this change. Most common type of barometers in use on board of the vessels are aneroid barometers. This type of equipment is measuring the atmospheric pressure without using any liquid. This instrument have small metal capsulated cell, usually made from copper, which is very flexible and even a small change in the atmospheric pressure cause the cell to expand or contract, and this actions cause an immediate change to the position of the arrow on the display. Barographs have one or usually few capsulated cells and gives information for pressure tendency which is a solid ground for forecasting the weather on board of the vessels. Thermometer is instrument for measuring of the air temperature. Changes in temperature along with other meteorological factors are used by mariners to compile more reliable predictions for the state of weather. Psychrometers consist of two thermometers “dry and wet”. They are used for measuring the air humidity. Dry thermometer is called dry-bulb and wet thermometer is called wet-bulb. Due to evaporation of water the wet-bulb always shows lower temperature than dry-bulb. Using this difference in the measurement and the relevant tables the OOW may calculate the relative humidity of the atmospheric air. The relative humidity is 100% when the readings of both thermometers match, and as bigger is the margin as drier is the air.

Nowadays, as a result of the progress made by meteorological specialist very important equipment for monitoring the weather parameters was invented. This equipment is called marine weather station (Fig. 9). It uses one or combination of sensors with very high resolution and gives information for: apparent wind direction and speed, air temperature, barometric pressure, relative humidity, wind chill and dew point. The latest models have options for external GPS and compass, which allows calculating true wind direction and speed. Also the latest models give reliable information and they are much more accurate than mechanical devices mentioned above. Using this fully automated equipment OOW will save valuable time because he shouldn’t measure every weather parameter manually, but the information is displayed on PC or NMEA data interface.

Fig. 6. Cup anemometer

Fig. 7. Electronic anemometer

Fig. 8. Aneroid barometer

Fig. 9. Marine weather station

4. CONCLUSIONS

Both systems Navtex and Inmarsat-C SafetyNet complement very well and provide mariners with timely and comprehensive weather information for the navigating area or for the areas in which the ship is about to enter. They provide the mariners with weather forecasts and allow them to choose the safest and most favorable route especially when sailing in winter and in open sea areas.

Mariners may take wrong decision, due to insufficient weather information. This could lead them to unsafe navigational waters. As a result of this environmental pollution may occur. Accidental spills of toxic, harmful materials, oils or oily compounds, and other raw materials are also possible sources of contamination of water (Grancharova V., I. Grancharov, 2013).

The assessment of all meteorological factors and bearing in mind of all information available on board will be in help for mariners to take the right decision in place to protect the ship and crew from natural disaster.

REFERENCES

[1]. WMO – ***Bulletin – The journal of the World Meteorological Organization,*** vol.58 (2) – April 2009, Geneva, Switzerland, 2009

[2]. IMO – ***SOLAS Consolidated Edition,*** London, England, 2009

[3]. IMO – ***NAVTEX Manual,*** London, England, 2012

[4]. Grancharova V., I. Grancharov - ***Sustainable port development in connection with environmental regulations***, Journal of Marine Technology and Environment, Vol. II/2013, ISSN 1844 – 6116, Constanta, Romania, 2013, p. 19-24

[5]. Shivarov A. – ***Practical hydromeorology,*** E-Litera Soft, Varna, Bulgaria, 2011.

NEW TECHNOLOGIES USED FOR AUTOMATION OF CONTAINER HANDLING AT TERMINALS

GRANCHAROVA VALENTINA

"Nikola Vaptsarov" Naval Academy, Varna, Bulgaria

Introducing of advanced and innovative technology for optimizing physical operations resulted from increased flow of goods through container terminals. The paper highlight about automatization in the terminals, which might lead to better productivity level, flexible work environment and effective utilization of resources. Many terminals are seeking the proper solutions for reducing the operational costs and providing an increased level of service to its customers. Information technology is now essential element of global economy. Container terminal operators are providers of container handling services and deals with the shifting of trend towards containerization of exports and imports. The efficient operation of a container terminal also depends on how efficiently it can process large volumes of information. Therefore the application of information technology to container terminal operations and management is critical to the success of the terminal. This will also include electronic data interchange of information between the terminal and its users. In this paper are proposed some decisions, concerning automation of process at terminals.

***Keywords**:* container handling, terminal operating system

1. INTRODUCTION

There is a big challenge for all IT Companies to design a solid manageable Terminal Operating System (TOS). The coordination of tasks in terminal, concerning of specialized equipment, technology, integration and facilitation the use of physical facilities and human resources, allows for a smooth container flow from the time the container arrives to the terminal until it is withdrawn by the consignee. An additional element has to ensure efficient container traffic within the terminal through a synchronized information flow, hence, to make sure the right information is delivered at the right time to those involved in the planning and operation of the container logistics.

2. METHODS FOR AUTOMATION OF TERMINAL PROCESSES

The overall task of a container terminal is to manage by a proper manner the processes, concerning vessel's berthing/unberthing, loading/discharging and storage of cargoes. The container terminals should provide sufficient area for transshipment from one type of transportation to another, as well as the temporary storage of containers. Most container terminals are interested in high throughout and short container dwell-times, since usually their main purpose is focused on transshipment of containers but not on their storage. The terminal operating system (TOS) often control the several subsystems, which are divided

according to the related operations and the equipment involved as follows: ship-to shore subsystem, waterside horizontal transport subsystem, storage subsystem and the hinterland subsystem (Stahlbock R., Voss St., 2008).

The *ship-to-shore subsystem* is designated to the loading and discharging operations of vessels. The problems related to ship-to-shore are connected to the stowage planning for deep-sea vessels, as well as berth and quay crane allocation for arriving vessels. The main aim of this system is the minimization of vessel's stay at the berth.

Some ports have find as a solution of this goal the performing of quay cranes remote control. Crane operation implemented from a remote control room improve also working condition for the operators while allows faster turning of the crane and as a result faster transshipment. The control room can be located near the terminal control room and in such manner to improve the communication between the all staff included. As negative of this technology can be pointed the need for minimization of the "out of service" period, which blocks the access to the quayside. Considering the latest spreader technologies, even 80–100 40 ft. containers may technically be handled per working hour (ABB Crane System, 2011).

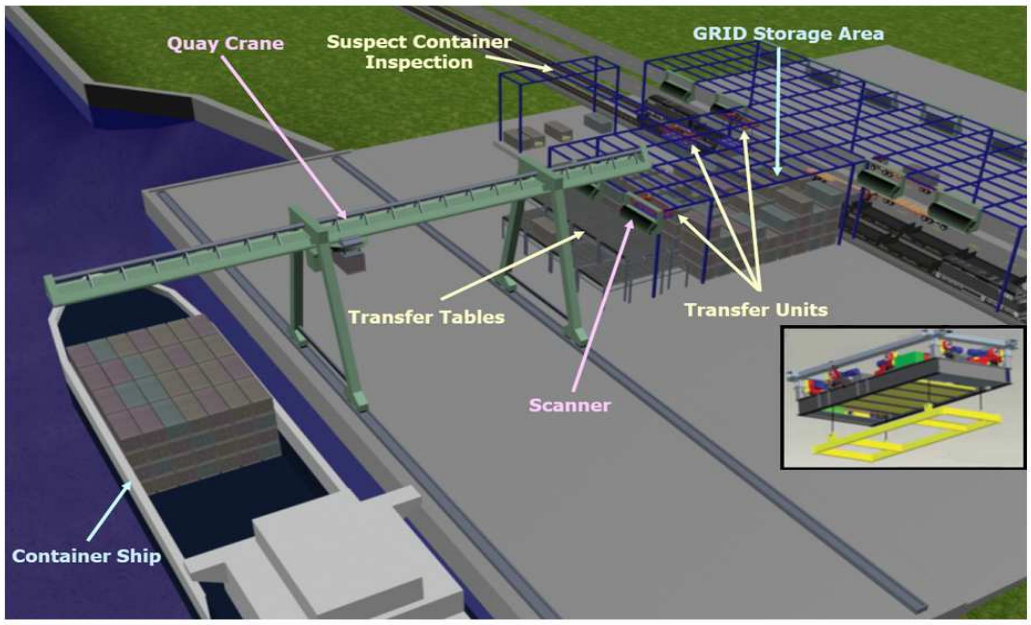

Fig. 1 Container terminal with GRID system

The cargo handling system Goods Retrieval and Inventory Distribution (GRID) was created by BEC Industries and work in several U.S. ports, among which is the port of Portsmouth, Virginia. This system performs easy verifying of container volume without further holding. Furthermore, it significantly reduces the number of unnecessary relocated container and allows simultaneous movement of incoming and outgoing containers and their storage in small area (up to 8 lines in height). Preliminary arrangement of containers (before ship's arrival at port) significantly reduces the time for vessel's stay (Fig. 1). The GRID system works on following manner: the gantry puts unloaded from ship container on a special conveyor belt system, the container have been registered from the system and guided to storage area or for direct loading on the land transport vehicles. The outgoing

containers are placed on the second conveyor belt and loaded by the quay crane on the vessel. Another great benefit of the system is that it might be powered by solar cells. Researchers from the University of Singapore are working on the system development in building comprehensive intermodal complex.

The *waterside horizontal transport* is the connection between ship-to-shore system and the storage subsystem. The general aims of this subsystem are efficient, smooth and fast transfer of containers between the quay cranes and the storage yard. In order to achieve these objectives, the right decisions on the type and the number of applied transport machines as well as on the scheduling and the routing of the machines have to be made.

Fig. 2 AGV fleet in the Port of Rotterdam, Netherlands

A modern container handling terminal require using of more and more automated technologies and reducing the number of working staff employed. Aspects like efficiency and impact on the environment sets difficult targets for engineering a terminal. The large container terminals like these situated in Rotterdam and Hamburg use automatically guided vehicles (AGV) for horizontal handling of containers in maritime terminals. The fleet of AGVs integrates yard-cranes and ship-cranes. The whole process is performed without direct human intervention (Fig. 2). The new generation of hybrid AGVs made from VDL could fully meet today's standards and requirements, with a focus on life cycle cost reduction, improved reliability and less impact on the environment. In October 2011 this AGV was delivered at the ECT Delta terminal in Rotterdam and after testing it was implemented. The hybrid AGV is capable of transporting ISO containers of 20 foot, 40 foot, 45 foot or two 20 foot containers at once. It is also able to handle loads up to 70 tons, and it can run at speed of up to 6 meters per second (VDL, 2011). The VDL AGV is built so that new techniques such as induction and hydrogen drives, or GPS navigation, can be incorporated in them without major modifications.

The importance of the storage subsystem has continuously grown over the last years along with the increasing traffic volume. The storage yards are usually divided into several blocks that consist of several bays, rows and tiers. The maximum stacking height (i.e., the maximum number of tiers) is limited by used stacking equipment. The storage area can be divided according to the destination of the containers (for vessel's loading, hinterland departure) and to the specific of cargo loaded (special areas for storage of empty, dangerous, damaged as well as for reefer or insulated containers) (Fig. 3).

The systematic choice of location and information exchange between equipment requires more exact rapid information networking than in the traditional container terminal in order to maximize the efficiency of container yard and safe handling and storing more containers in time due to the large size of container ships. Implementation of TOS database programs automate the handling of all assets in the terminal based on manual entry of container and truck numbers. This automation is essential for rapid handling of containers which are coming IN and OUT through the gate.

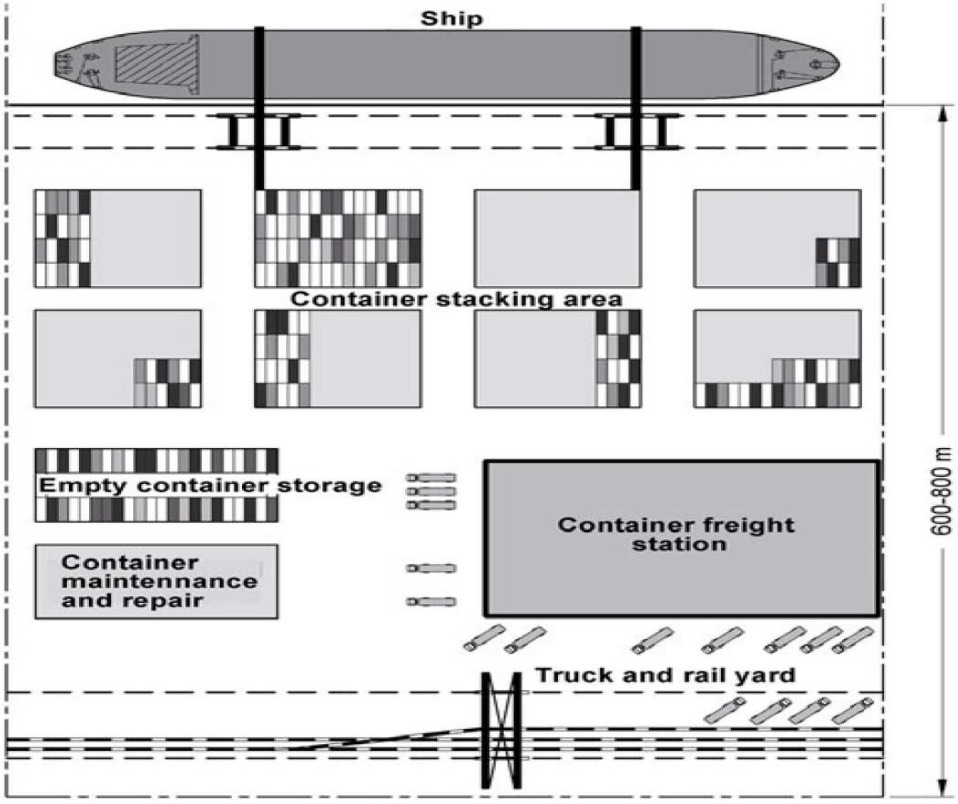

Fig. 3 General layout of container terminal

Due to the fact that more container terminal operators recognize the need for improved asset visibility and control, especially within automated container handling processes for accurate real-time accounting of the incoming, outgoing and existing cargo units, optical character recognition (OCR) is often one of the lowest cost means for achieving of these targets. OCR provides a reliable method of identification, without requiring application of any tag or device to the asset that also includes a visual record of the asset at the time of

reading. Common OCR applications for terminal automation include the following systems: Gate OCR system (for portal and pedestal gates), Crane-mounted OCR systems (Quay crane, RTG, MTG and other CHE's), Rail Operations (rail portal gates) and Yard Operations (Moving Inventory Vehicles, utilizing integrated OCR and GPS systems). Hi-Tech Solutions has recently commercialized its container code recognition (CCR) systems for portal and pedestal gate applications and crane applications. Since the container markings follow an ISO international standard, the CCR systems can be installed in any location worldwide.
A CCR system can generally be divided into 3 general modules: image-capturing units (including illumination devices); a software recognition engine and application programs; system infrastructure, (mounting and support structure and communication network). New opportunities for OCR at a traditional container terminal include vessel and yard operations where equipment is identified at key points of work such as with quayside ship-to-shore (STS) cranes, as well as at handoff points to gantry cranes operating in the container yard and train areas.

In search process optimization modern containers terminals are equipped with GPS (global positioning system) for controlling of container's movement. The GPS receivers used at terminals has to define the exact position of units (container or vehicle) with accuracy from 10 to 30 cm. On Figure 4 is shown the block scheme for GPS controlling of container units at terminals like container terminal in Melbourne Mourepiane terminal in Marseille and many other container terminals in Singapore, Rotterdam, Hamburg. Positions that resulted in GPS receiver is submited to GPS console, which registers and sends each movement to a central computer. Network controller processes the whole system and switches transceivers in server center and terminal machines. Systems usually allow two-way communication, which is very useful when the terminal machine is moving. The signal sent from the computer terminal, is accepted by the modem of the terminal machine and transferred to the processor, which processes it and give the appropriate command to the operator or directly to the machine.

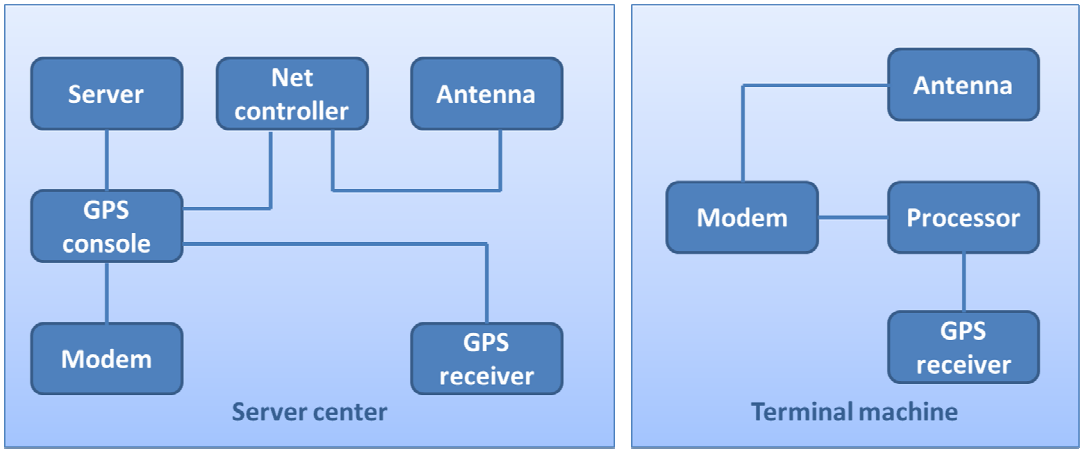

Fig. 4 GPS system for container movement at terminal

The results of researches show that the lower operation frequency of the GPS system is more reliable and is not affected by interference in the presence of barriers between the antenna of terminal operations center and antenna, placed on the terminal machine. The most used frequency is 900 MHz (preferable than 1.8 GHz and 2.4 GHz). Trucks, RTG or

AGVs are terminal machines. Terminal spreaders are not used in such systems, because the accuracy of the interference of the system greatly deteriorated.

Radio Frequency Identification (RFID) has been successfully used in transportation and manufacturing since the mid-80s and its use is growing rapidly as the costs come down and the benefits are recognized. The primary advantage of RFID in a port/terminal application is that it is an “automatic” data collection technology. Whereas other forms of data collection, whether bar code or manual methods, depend on employees to record information, RFID relieves them from this time-consuming and error-prone process. The two direct benefits of this are: accurate and complete data collection and better utilization of employees’ time. Security at port area can be significantly enhanced with the use of RFID. The RFID-aided harbour container tracing and customs clearance system is a management system based on active RFID electronic label, combined with EDI, and integrated the container transportation process and container customs clearance process.

OCR and RFID technologies are very important for supporting the required information flow that coordinates the different tasks and processes. Figure 5 shows how the flow of information must be embedded with the container terminal operation to reach a smooth traffic flow (Narsoo J., W. Muslun, and M. S. Sunhaloo, 2009).

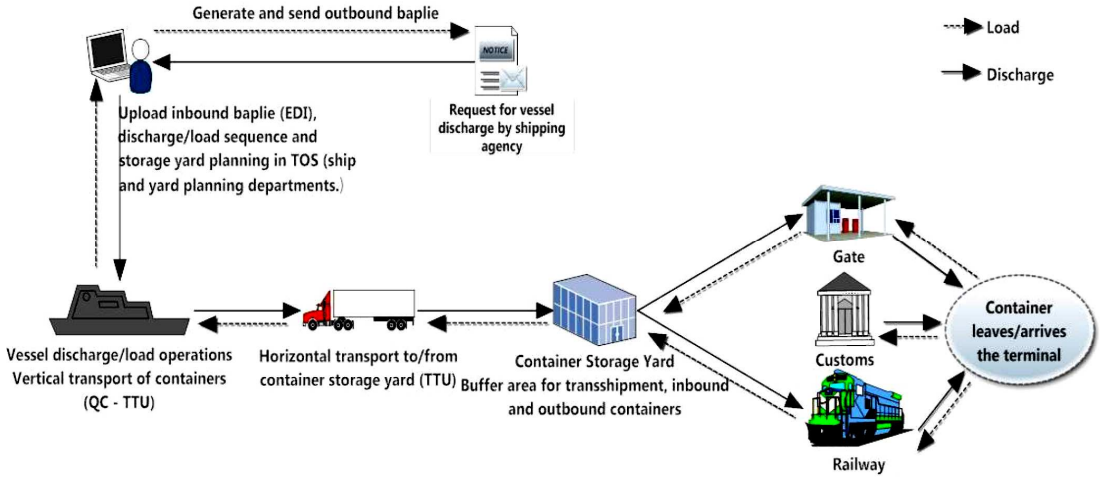

Fig. 5 Information exchange at container terminal

The application of optical character recognition (OCR) in ports began in Asia in 1998 with the deployment of the first test systems for Shanghai United Asia Container Depot. As computing power increased and system accuracy and automation rates improved, adoption rates slowly increased as well in Asia, Europe and the USA. Today, OCR system installations in total are over 1700 worldwide with the overall OCR turnover in ports. The actual OCR installations till 2011 at worldwide ports count 1736. The US region leads with 790 OCR installations, followed by Asia Pacific - 544, Europe - 244, Middle East - 80, Latin America - 51 and Africa - 27. On Figure 6 is shown percentage division of OCR installation by type according to the official statistic of PEMA.

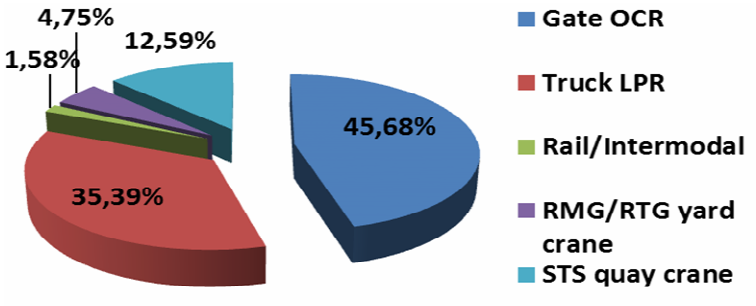

Fig. 6 Percentage division of OCR installation by type as per PEMA

Innovative technology RFID (radio frequency identification) is a method for automatic identification of objects in which the identifier (a label tag, card, keychain, sticker, etc.), located on the cargo is reading or writing data using radio waves. Radio frequency identification (RFID) is successfully applied for the treatment of a large number of standard and specialized containers from port operators and customs authorities in major container ports. By using of RFID system each port entry and exit or any movement of cargo handling equipment is comprised of RFID reader and antenna (Fig. 7)(Grancharov I., V. Grancharova, 2013). The identifier may be secured to a container and with the aid of a suitable control software to record its movement.

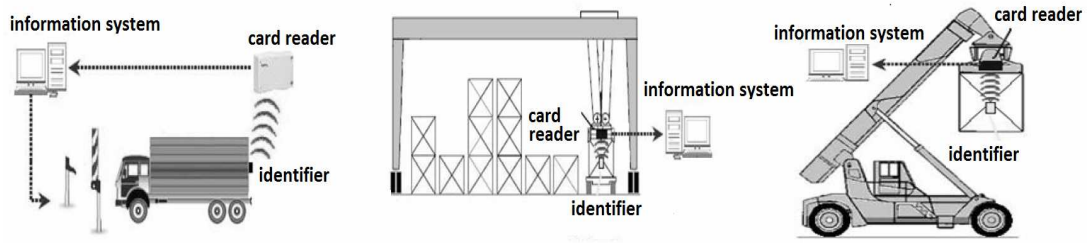

Fig. 7 Automatic identification of containers using RFID

Recorded identifier data can be read and modified by the reader, then the information is transmitted to a computer for processing and taking further action (eg. to be operated doors, barriers or other device). The use of RFID tags for recording the location of containers and monitoring the location and activities of yard vehicles will improve the overall quality of data and, therefore, the efficiency of the entire operation. This provides managers with an up-to-the-minute picture of activities and that, in turn, allows them to respond to developing situations in a timely manner.

3. CONCLUSIONS

Transportation technology and equipment for container handling terminals are evolving constantly. The increased flow of goods through container terminals requires continuous improvement of the organization and planning of container handling in order to optimize additional movements at the terminal to load a container in a particular item to ship.

Maritime container terminals are now faced with higher volume of traffic, limited land, larger vessel sizes, and lower profit margins. Nowadays the European Container Terminal (ECT) in Rotterdam, the Netherlands is the most automated container terminal in the world.

The arisen volume of containerized goods and necessity of rapid handling, especially through portal entry/exit gates lead to introducing of Terminal Operating System (TOS) in most large terminals. For the quay side container handling crane, the main objection to achieving the automation is that the relative position of the ship to the crane could not be surely recognized due to the ships rolling motion, etc. Transfer cranes in the container stock yard do not face to ships and their automation, which is in a relatively easy environment compared with the quay side container cranes.

GRID system performs direct scanning or security check, which increases from 2 to 3 times the capacity of the terminal storage area.

During their implementation at marine terminals AGVs has been subject of substantial improvement in speed, as well as in the navigation technology and communications systems. Rapid growth in container traffic and the associated threat of cargo handling gridlock are driving the development of automated solutions for terminal logistics. Their main benefits are: improved productivity reduced wage and operating costs, increased safety, predictable, continuous operation almost completely independent from the weather, maximum use of space and resource-saving operation.

The application of OCR technology has so far been leveraged to deliver benefits including labor productivity, safety and security and increased asset and port utilization. A key additional driver of growth in the port community and marine terminal market today is environmental sustainability. The company Hi-Tech Solutions offers solutions with standard interface for data and images, concerning implementation of OCR systems for gate, rail and crane operations. Every phase is monitored and the traceability of truck, driver and containers is easy.

Real-time identification of containers and chassis using optical character recognition, radio-frequency identification and GPS is one good solution for reducing 3 - 4 time the gate traffic queues associated with slow transshipment and for guiding of container's movement.

REFERENCES

[1] ABB Crane System - ***Remotely controlled STS crane***, Port Technology N. 52/2011 London, 2011, p. 42-43

[2] Grancharov I., V. Grancharova - ***Innovative decisions for improving port efficiency in container handlin***g, Science & Technologies, Vol. III; No.2/ 2013 Nautical & Environmental studies, St. Zagora, 2013, p.14-18

[3] Narsoo J., W. Muslun, and M. S. Sunhaloo - ***A Radio Frequency Identification Container (RFID) Tracking System for Port Louis Harbor: The Case of Mauritius***. Issues in Informing Science and Information Technology, Vol. 6, 2009, p.127-142

[4] Stahlbock R., Voss St. - ***Operations research at container terminals***, Springer- Verlag, 2008

[5] VDL, ***Upgrading to automated guided vehicles***, Port Technology N. 52/2011, London, 2011, p.70-71

ANALYSIS OF SHIP OPERATION FOR A CONTAINER TERMINAL

[1]LOKE K.B., [2]A.H. SAHARUDDIN, [3]A.R. IBRAHIM, [4]I. RIZAL, [5]A.S.A.KADER, [6]A.M.ZAMANI

[1,2,3,4,5,6]*School of Maritime Business and Management Universiti Malaysia Terengganu, Malaysia*

This study is looking for delay factors of ship operation in a container terminal. Ship operation is a complex process that is affected by many factors, such as weather delays, vessel delays and stevedore delays. These factors will slow down the handling performance and increase the handling time and cost. Hence, secondary data is collected from Malaysian Port and analysis by SPSS. Correlation and pie chart are used to analysis and display the result. The initial result showed that the main cause of delay is stevedore delays (82.60%) and have high correlation with berth turnaround time (0.831). This study further analysis stevedore delays; the results showed that waiting for prime mover is the main delay factor, which contributed to about 41.2% that affected the performance of ship operation. It also has high correlation with berth turnaround time (0.716). Therefore, this study concluded that the stevedore delays and waiting for prime mover is the main cause of delay in ship operation in a container terminal.

***Keywords**:* delay factors; ship operation; container terminal; stevedore delays; prime mover

1. INTRODUCTION

A lot of study looked into handling efficiency issues in container terminal. They aim to improve the handling rate by simulation, mathematics and empirical. But, the studies did not look into delay factors of operation. Therefore, this study intended to overcome the shortcoming by analysis the sources of delay factors that affected ship operation in a container terminal.

2. LITERATURE REVIEW

When a container vessel arrived at the container terminal, the containers on board would be unloaded from the vessel. This task is handled by quay crane (QC). After that, the containers are transferred from the QC to prime mover (PM), which would carry the containers from the berthing area to the stacking area. Next, the rubber tyred-gantry crane (RTG) or straddle carrier (SC) arranged the containers in the storage area. The containers must be stored in a manner that would minimize the time taken to retrieve the containers. For export containers, the prime mover would carry the containers from container yard to berthing area for loading. Thereafter, the container vessel would carry the containers departed from the port (Iris and Rene, 2002). For export and import of containers, they would passed by entry gate and custom clearance. Some of the containers would store and repackaging in container freight station, mostly is for consolidation shipment.

Therefore, there are four main operation systems in container terminal; such as ship operation, quay transfer operation, container yard operation and receipt/delivery operation. In terminals that have Container Freight Station (CFS) would have fifth system that is CFS operation (Thomas et al, 1994). It indicated that the terminal operations involve many interactions (Koh et al, 1994). In the real container terminal system the interactions are the critical issues; some of the principal aspects involve with interference among dock cranes, interference among yard cranes, interference among connections units, interference among containers themselves, access problems and other interactions and externality (Bruzzone et al, 1999).

Most of the studies increased the ship operation efficiency by work schedule, simulation and empirical study. The efficiency of ship operation depended primarily on the smooth and orderly process of handling containers, especially during scheduling of ship's loading process (Akio et.al, 2002). The process of ship operation is operated by quay cranes along their respective berths. The discharge process must be implemented before the loading process when the tasks handle in the hold of same ship bay (Kim and Park, 2004).

The ship operation handling by cargo-handling equipment has capability to achieve faster handling rate. It associated with high handling rate of TEU throughput per quay crane which gives large savings in stevedoring costs. Ship operation required equipment that works continuously with moderate maintenance effort and deploys in a variety of roles to suit changing traffic demands (Branch, 1986). So that, the selection of suitable handling equipment is important to support the operation requirement.

The management of ship operation consists of berth allocation, stowage planning and logistics planning (Won and Yong, 1999). Berth allocation controlled the loading and unloading of the ship's containers. Stowage planning assigned storage locations to the containers in the vicinity of the ship. Logistics planning assigned and coordinated the operations of the container handling equipment such as gantry cranes, transfer cranes and yard tractors in the transportation of containers between the ship's bay and the container yard. A well manage of operation would minimize the ship's waiting time and thereby maximizes the utilization of container terminal resources.

This paper emphasized on the delay factors on ship operation which did not highlighted in previous studies. It aims to analyst the factors that affected the ship operation performance and by then to increase the handling performance of the operation.

3. METHODOLOGY

An extensive secondary data collected from operation and statistic departments of Malaysian Port. The secondary data are based on ship operation delay parameters. Major types of information what were secured from these secondary sources include berth turnaround times, stevedore delays, vessel delays, weather delays, waiting discharge plan, crane breaks down, hatch closing, shift change, unlashing/lashing, waiting prime mover, system failures, crane booms up, and out of gauge. The secondary data used for ship operation delay analyses. Statistical Package Social Science (SPSS) used for statistical analysis purpose. Secondary data were checked for normality and reliability test. Normality test is important to determine the applying statistical techniques (McClave et.al, 2001). The significance level is 0.05 (Siegel and John, 1988). Reliability test used to check for the accuracy of data collected. Alpha value above or equal to 0.6 can be assumed as good and

acceptable (Abu and Tasir, 2001). Consider the population of data that is non-normal distribution, Spearman Correlation is selected to test for the relationship. The r-value is equal of above 0.7 is acceptable (McClave et.al, 2001). Then, the results were presented using Spearman Correlations and pie chart.

4. RESULT AND DISCUSSION

4.1 ANALYSIS ON NORMALITY TEST

Table 1 shows normality test for ship operation. A low significance value 0.000 indicated that the data differs significantly from a normal distribution.

Table 1: Normality test for ship operation

	Kolmogorov-Smirnov[a]		
	Statistic	**df**	**Sig.**
Berth Turnaround Time	0.095	1610	0.000
Stevedore Delays	0.176	1610	0.000
Vessel Delays	0.316	1610	0.000
Weather Delays	0.519	1610	0.000
[a.] Lilliefors Significance Correction			

4.2 ANALYSIS ON RELIABILITY TEST

Table 2 showed the alpha value for ship operation is 0.6330. Since it is above 0.6, it is acceptable.

Table 2: Ship operation reliability analysis

Reliability Coefficients	
Item	**Value**
No. of Cases	1610
No. of Items	4
Alpha	0.6330

4.3 ANALYSIS ON CORRELATIONS

Table 3 showed the Spearman correlations analysis for ship operation. Result from table 3 showed that stevedore delays with an r-value of 0.831, at two-tailed p-value of 0.01, can be concluded that the correlation coefficient is significant beyond the 1 per cent level. On the other hand, the r-values of vessel delays and weather delays are 0.625 and 0.147 respectively. Referring to Guilford's rule of thumb correlations, stevedore delays have a high correlation with berth turnaround times (BTT) but vessel delays (VD) have a moderate correlation with berth turnaround times and weather delays (WD) have an almost negligible relationship with berth turnaround times (Aziz, 2005; Guilford, 1956).

Table 3: Spearman correlations analysis for ship operation

			Berth Turnaround Time
Spearman's rho	Berth Turnaround Time	Correlation Coefficient	1.000
		Sin. (2-tailed)	-
	Stevedore Delays	Correlation Coefficient	0.831*
		Sin. (2-tailed)	0.000
	Vessel Delays	Correlation Coefficient	0.625*
		Sin. (2-tailed)	0.000
	Weather Delays	Correlation Coefficient	0.147*
		Sin. (2-tailed)	0.000
* Correlation is significant at the 0.1 level (2-tailed)			
[a.] Listwise N = 1606			

This study further analysis stevedore delays. Table 4 shows the Spearman correlations analysis for stevedore delays on ship operation. Result from Table 4 indicates that shift change (SC), waiting for PM (WP) and hatch closing (HC) show r-values of 0.828, 0.716 and 0.713 respectively. It is significant at two-tailed p-value of 0.01, and can be concludes that the correlation coefficient is significant beyond the 1 per cent level. Therefore, shift change, hatch closing and waiting for PM have a strong correlation with berth turnaround times. On the other hand, crane breaks down (CB), unlashing/lashing (UNLS) and waiting discharge plan (WD) shows r-value of 0.534, 0.504 and 0.503 respectively. All are moderately correlate with berth turnaround times. Out of gauge (OOG) and crane booms up (CU) with r-value 0.374 and 0.281 respective are shown in table 4. Both are weakly correlate with berth turnaround times. For system failures (SF), the r-value is -0.012 though the significant value is 0.620 (above 0.05). It indicates that the correlations between berth turnaround times and system failures are not significant, and the two variables are not linearly related.

For Spearman correlations test, the variables would be acceptable if the r-value is equal or above 0.7. Therefore, shift change (SC), waiting for PM (WP), and hatch closing (HC) are accept which show significant relationship with berth turnaround times. Besides, crane breaks down (CB), unlashing/lashing (UNLS), waiting discharge plan (WD), Out of gauge (OOG), crane booms up (CU) and system failures (SF) are reject which shown not significant relationships between berth turnaround times.

According to usual sequence, shift change, waiting for PM, hatch closing, crane breaks down, unlashing/lashing, waiting discharge plan, out of gauge, and crane booms up show a positive relationship, although some show a weak relationship. However, system failure shows a very weak non-significant negative relationship, it may be cause by a few cases happening during the operation.

Table 4: Spearman correlations analysis for stevedore delays on ship operation

			Berth Turnaround Time
Spearman's rho	Berth Turnaround Time	Correlation Coefficient	1.000
		Sin. (2-tailed)	-
	Out of Gauge	Correlation Coefficient	0.374*
		Sin. (2-tailed)	0.000
	Waiting Discharge Plan	Correlation Coefficient	0.503*
		Sin. (2-tailed)	0.000
	Crane Breaks Down	Correlation Coefficient	0.534*
		Sin. (2-tailed)	0.000
	Hatch Closing	Correlation Coefficient	0.713*
		Sin. (2-tailed)	0.000
	Shift Change	Correlation Coefficient	0.828*
		Sin. (2-tailed)	0.000
	Unlashing/Lashing	Correlation Coefficient	0.504*
		Sin. (2-tailed)	0.000
	System Failures	Correlation Coefficient	-0.012
		Sin. (2-tailed)	0.000
	Waiting for PM	Correlation Coefficient	0.716*
		Sin. (2-tailed)	0.000
	Crane Booms Up	Correlation Coefficient	0.281*
		Sin. (2-tailed)	0.000
* Correlation is significant at the 0.1 level (2-tailed)			
[a.] Listwise N = 1606			

4.4 ANALYSIS ON PIE CHART

Figure 1 shows pie chart analyses for ship operation. It shows that stevedore delays, vessel delays and weather delays are 82.6%, 17.1% and 0.3% respectively. Most of the time, stevedore delays are shown to be the main delay factor at container terminal during the ship operation. The second delay factor is shown to be vessel delays and the third delay factor is shown to be weather delays. To analysis further the relationship between the 3 delay factors with berth turnaround times, correlation test was done and this is done in the next section.

Then, it further analyst on stevedore delays. Figure 2 shows the total percentage of stevedore delay cases that happen during the ship operation. Waiting for PM 41.2%, hatch closing 29.4%, shift change 10.3%, out of gauge 6.9%, crane breaks down 5.9%, waiting discharge plan 3.9%, unlashing/lashing 1.8%, crane booms up 0.7% and system failures 0.0%. Initial finding reveals that waiting for PM is the main delay factor, hatch closing is the second delay factor, and shift change is the third delay factor during the ship operation.

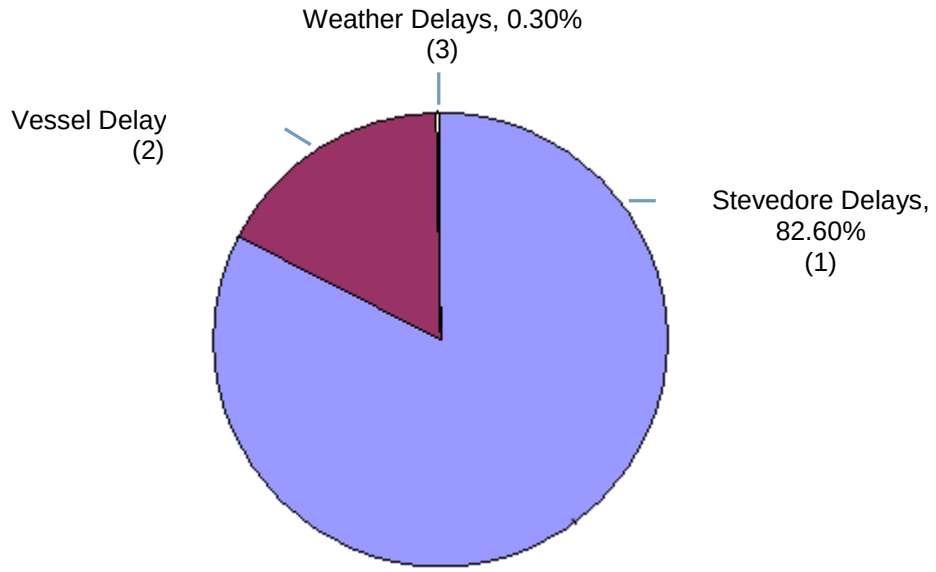

Fig. 1. Pie chart analyses for ship operation

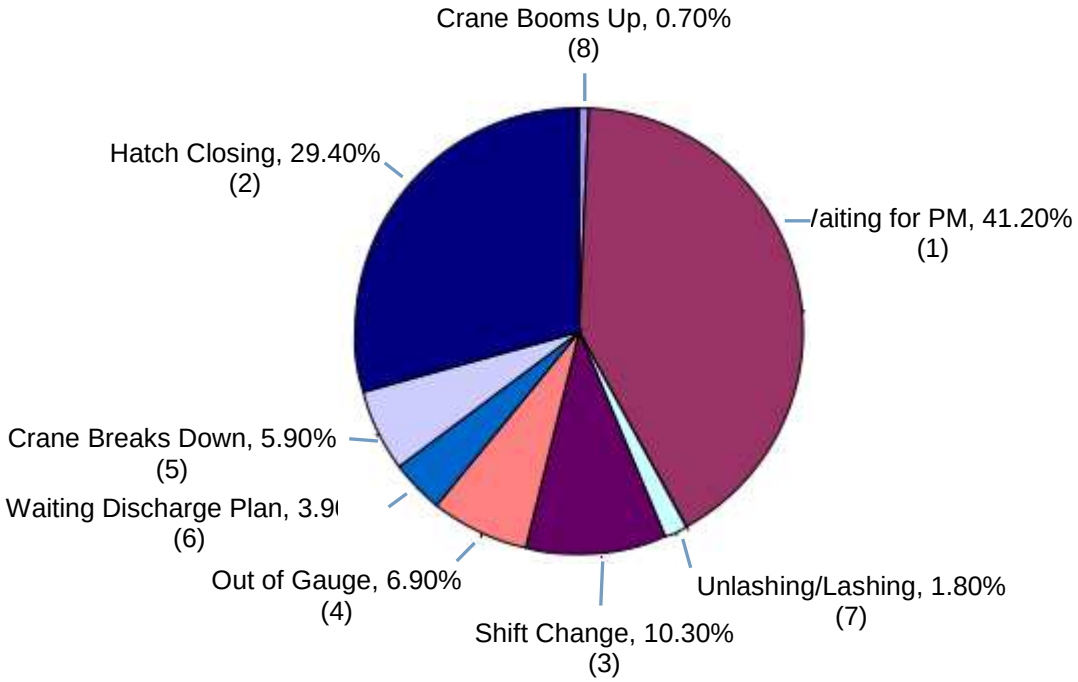

Fig. 2. Pie chart analyses for stevedore delays (sub-items)

5. CONCLUSIONS

Stevedore delay is the main source of delays in ship operation. The significant r-value is 0.831 (table 3), a high correlation relationship with berth turnaround times. In addition, 82.6% of ship operation delay is caused by stevedore delay. Stevedore delays consist of nine sub-items; out of gauge, waiting for discharge plan, crane breaks down, hatch closing, shift changes, unlashing / lashing, system failures, waiting for PMs, and crane booms up. Shift change (0.828), hatch closing (0.713) and waiting for PMs (0.716) have strong correlation relationships with BTT (table 4). Besides, waiting for PMs caused 41.2% of stevedore delays. This percentage is highest among the nine sub-items. Hence, the time spent for waiting for PMs must be solved to try to reduce the immobile times between QC and PMs. The second cause of stevedore delays is hatch closing (29.4%) and the third is shift changes (10.3%). The results showed that waiting for vehicles as the main delay factor on ship operation. Therefore, attention might be paid to vehicles and machinery co-ordination. So, adjustments must be made from time to time based on demand. For example, by increasing or decreasing the vehicles and machinery from one site to another as demand varies according to time and space. The performances of the terminal operation determines by a combination of vehicles and machinery components.

ACKNOWLEDGMENTS

We extend our sincere appreciation and indebtedness to Malaysian Port operation department, statistics department, human resource department, and technical department for the guidance, support and encouragement. We extend our sincere appreciation and indebtedness to UMT and their funder for the guidance, support and encouragement. We would also like to thank the reviewers of this paper for they helpful suggestion.

REFERENCES

[1]. Abu, M.S. and Tasir, Z. - ***Pengenalan kepada Analisis Data Berkomputer SPSS 10.0***, Venton Publishing, Kuala Lumpur, pp. 299, 2001

[2]. Akio, I., Etsuko, N., Stratos, P., and Kazuya, S. - ***The Containership Loading Problem***, International Journal of Maritime Economics, 4(2), June2002, pp. 126-148, 2002

[3]. Aziz, W.A. - ***Relationship between Two Variables. Describe and Predict Relationship between Variables***, Notes for Research Method and Data Analysis Workshop 2005, Faculty of Management and Economics, College University Science and Technology Malaysia (KUSTEM), 31st March -2nd April 2005, pp. 10, 2005

[4]. Branch, A.E. - ***Elements of Port Operation and Management***, Chapmen and Hall Ltd., New York, pp. 240, 1986

[5]. Bruzzone, A.G., Giribone, P., and Revetria, R. - ***Operative Requirements and Advances for the New Generation Simulators in Multimodal Container Terminals***, Proceedings of the 1999 Winter Simulation Conference, pp. 1243-1252, 1999

[6]. Iris, F.A.V. and Rene, D.K. - ***Transhipment of Containers at a Container Terminal: An Overview***, European Journal of Operational Research, Volume 147, Issue 1, 16 May 2003, pp. 1-16, 2002

[7]. Kim, K.H. and Park, Y.M. - ***A Crane Scheduling Method for Port Container Terminals***, European Journal of Operational Research, 156(3), 1 August 2004, pp. 752-768, 2004

[8]. Koh, P.H., Goh, J.L.K., Ng, H.S. and Ng, H.C. - ***Using Simulation to Preview Plans of a Container Port Operation***, Proceedings of the 1994 Winter Simulation Conference, Orlando, Florida, December, 1994

[9]. Guilford, J.P. - ***Fundamental Statistics in Psychology and Education***, McGrawv-Hill, New York, pp. 145, 1956

[10]. McClave, J.T., Benson, P.G. and Sincich, T. - ***Statistics for Business and Economics***, Prentice-Hall, Inc., Upper Saddle River, New Jersey 07458, pp. 1028, 2001
[11]. Thomas, B.J., Roach, D.K., Interface4 Ltd, and International Labour Office - ***A Project by the International Labour Office (ILO),*** Financed by the Royal Government of The Kingdom of The Netherlands, Port Development Programme, C.1.1 Container Terminal Operations, pp. 56, 1994
[12]. Siegel, S. and John C.N. - ***Nonparametric Statistics for the Behavioral Sciences***, Second Edition, McGraw-Hill, United States of America, pp. 399, 1988
[13]. Won, Y.Y. and Yong, S.C. - ***A Simulation Model for Container-Terminal Operation Analysis Using an Object-Oriented Approach*** , International Journal of Production Economics, 59(1-3), March 1999, pp. 221-230, 1999

CONSIDERATIONS ON THE PERFORMANCE OF SINGLE VAPOR COMPRESSION CYCLES WITH SUPERHEATING AND WITHOUT SUBCOOLING

MEMET FEIZA

Constanta Maritime University, Romania

In this paper it is evaluated the global performance of an one stage vapor compression cycle with superheating and no sub cooling, calculated as the ratio between refrigerating capacity and electrical power supplied to compressor (COP). It is stated that the superheating of the refrigerant in vapor state occurs inside the refrigerant space. This phenomenon is spontaneous and useful for the protection of the compressor.
Since the ban of Hydrochlorofluorocarbons (HCFCs), Hydrofluorocarbons (HFCs) are used as alternative, one of the most visible in marine refrigeration being the non ozone depleting R134a.
But the environmental issue does not only include the ozone layer; there is also an increasing worry about the global warming potential due to greenhouse effect.
This is why the objective of this work is oriented on the performance of an one stage vapor compression cycle working with R134a and two more refrigerants, having lower GWP. These are R290 and R152a.
The analysis for specific conditions will reveal that even if R152a has higher GWP than R290, its COP is better than R134a and R290.

***Keywords**:* vapor compression, superheating, performance, environment

1. INTRODUCTION

Food processing and cold storage represent important applications of refrigeration for preserving and distributing perishables at optimum nourishing level.

These refrigeration subsectors play important roles in the economy of developing and developed countries (IPCC/TEAP, 2005).

For the long-term storage of frozen food are used temperatures in the range ($-15^oC \div -30^oC$) and for chilled goods are used for their cooling and storage temperatures between ($-1^oC \div -10^oC$).

The main technologies met in food processing and cold storage are based on reciprocating compressors. In their cycles are working refrigerants as ammonia, HFCs or HCs.

Marine transport refrigeration needs refrigeration plants able to transport chilled or frozen goods. On board of fishing vessels should be assured also fish processing.

The role of a transport refrigeration system is to maintain the temperature constant during transport, according to the type of good.

Refrigeration systems on board the ships have to be compact, lightweight, robust, sturdily built to withstand movements during sailing; also they should be able to work in a wide range of exterior temperatures and variable weather conditions.

Still, refrigerant leakage occurs. It is needed that refrigerant and spare components exist on board the ships. Also, it is mandatory to be ensured a safe operation with working fluids, especially for ships where options for evacuation are limited.

Maritime refrigeration has also other goals: specialized tankers are used to carry liquefied gases, specially liquefied petrol gas (LPG) and liquefied natural gas (LNG). Medium and large LNG tankers are used to transport LNG at normal pressure.

For such kind of transport, the refrigeration effect is assured by LNG evaporation which is recondensed in special refrigeration units.

Refrigerated containers permit continuous storage during transport on different types of mobile platforms.

These can be porthole containers or integral containers. The first ones are old type; they are insulated, present two front apertures and do not have built-in refrigeration plants. Integral refrigerated containers are new concept and have their own refrigeration system.

R134a is a refrigerant traditionally used in single stage refrigeration systems on board the ships. Because of its high GWP, future legislation will encourage the replacement of R134a with more environmental friendly refrigerants.

In the following, a comparative analysis of a single stage refrigeration cycle with superheating and no sub cooling it is presented; the superheating of vapor refrigerant occurs inside refrigerated space. Results are obtained for three working fluids: R134a, R290, R152a.

2. CONSIDERATIONS ON ECO-FRIENDLY REFRIGERANTS

In marine refrigeration, CFCs and HCFCs have been traditionally used, but because of their negative effect on environment their use is under international restriction.

Legally, care about the ozone layer is taken into account by the Montreal Protocol (1987), while international concern about global warming was stated by Kyoto Protocol (1997).

CFCs and HCFCs are responsible for damages in the ozone layer and for climate change.

Because HFCs do not contain chlorine and have null Ozone Depletion Potential (ODP), they are alternatives for old refrigerants in marine refrigeration (Harbach, 2005).

Still, refrigerants belonging to this family show a quite high Global Warming Potential (GWP).

The presence of fluorine, atoms in R134a (HFC 134a) is the reason for the important environmental impact assessed by GWP, with major consequences on the future development of refrigeration application (Baskaran and Mathews, 2012).

HFCs might be replaced by HCs, which are also chlorine and fluorine free and present GWP lower than the ones of HFCs.

This study is one of the efforts made to find low GWP candidates, able to be used in single stage vapor compression systems.

In Table 1 are given some properties of R134a (HFC 134a) and alternative refrigerants R290 (HC290) and R152a (HFC152a), resulting deviations from values of R134a (Paroche and Gupta, 2012).

Table 1: Same thermodynamic and environmental features of considered refrigerants

Refrigerant	Molecular weight, g/mol	Boiling temperature, ^{o}C	ODP	GWP
R134a (HFC 134a)	102	– 26,1	0	1300
R290 (HC 290)	44,1	– 42,0	0	20
R152a (HFC 152a)	66	– 24,0	0	140

3. THERODYNAMIC ANALYSIS OF A VAPOR COMPRESSION REFRIGERATION SYSTEM

In Figure 1 it is given a vapor compression system with superheating. The parts of such a system are: compressor, condenser, expansion valve and evaporator. As seen in the representation, the goal of the refrigeration system is to remove heat from one area and transfer it to a different location.

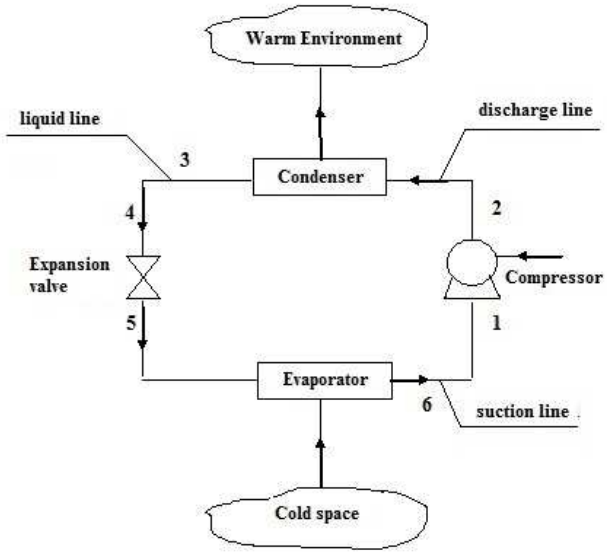

Fig. 1. Single – stage vapor compression system representation

A low pressure and temperature liquid, known as “refrigerant”, is turned into vapor in the evaporator, by absorbing heat from the cold space and keeping that space cool. The working fluid is driven around the refrigeration cycle by the compressor. Its role is to compress the low pressure and temperature vapors leaving from the evaporator. Resulted high pressure and temperature vapors are condensed in the condenser by rejecting heat to the surrounding environment.

The high pressure and temperature liquid resulted from the condenser is cooled and reduced in pressure by leading it through the expansion valve. With this new state, the refrigerant is introduced in the evaporator.

Vapors leaving the evaporator are in saturated state. Superheating is given by the temperature difference between compressor inlet temperature and evaporator saturation temperature (Kilicarslan and Kurtbaş, 2011).

The superheating during running of the system is needed in order to assure a refrigerant without liquid droplets at the compressor inlet, fact that will protect the compressor against damages.

The superheating of a refrigerant might happen in the last section of the evaporator or in the suction line. In the refrigeration system under analysis superheating is a spontaneous process.

It is considered that superheating happens in the suction line, which is located inside the cold space and also, no sub cooling and pressure drop occur in the refrigeration cycle.

The isentropic work input to compressor for superheating situation, is given by:

$$W_{c,sh} = m_r \left(h_2 - h_1\right) \tag{1}$$

where m_r is the refrigerant mass and h_1/h_2 are specific enthalpies at the inlet / outlet of the compressor).

For m_r = 1 kg, the specific work of compression is:

$$w_{c,sh} = h_2 - h_1 \tag{2}$$

The specific refrigeration effect is written as:

$$q_{evap,sh} = h_1 - h_5 \tag{3}$$

The enthalpy of superheated refrigerant vapors, h_1, is expressed by the help of enthalpy of saturated refrigerant vapors for the state of leaving the evaporator, h_6; also, are involved the specific heat of the refrigerant in vapor state, c_p, the evaporation temperature, T_0 and the temperature at the compressor inlet, T_1. Thus:

$$h_1 = h_6 + c_p \left(T_1 - T_0\right) \tag{4}$$

In the expansion valve, the process is isenthalpic, so, for enthalpies before and after this device:

$$h_4 = h_5 \tag{5}$$

The performance of the refrigeration cycle is evaluated by the Coefficient of Performance (COP), on the basis of the first law of thermodynamics (Bolaji et al, 2011), therefore:

$$COP_{sh} = \frac{q_{evap.sh}}{w_{sh}} \tag{6}$$

Above, w_{sh} is the specific actual work, defined by:

$$w_{sh} = \frac{w_{c,sh}}{\eta_s} \tag{7}$$

where η_S is the isentropic efficiency.

It can be assessed by the bellow formula, where p_c and p_0 are condensation and evaporation pressures, k is the adiabatic index and η_p is the polytropic efficiency. So:

$$\eta_s = \frac{\left(\frac{p_c}{p_0}\right)^{\frac{k-1}{k}}}{\left[\left(\frac{p_c}{p_0}\right)^{\frac{k-1}{k\eta_p}} - 1\right]} \tag{8}$$

4. RESULTS AND DISCUSSION

From Figure 2 it is possible to see the dependency between COP and evaporation temperature (T_0), when condensation temperature (T_c) is kept constant, for the single stage refrigeration cycle with a given superheating (ΔT_{sh}), no sub cooling and a specific polytropic efficiency (η_p).

The evaporation temperature takes values in the range ($0^oC \div 40^oC$), while the condensation temperature is fixed at 48^oC, the considered superheating degree is 4^oC and the polytropic efficiency is 0,9.

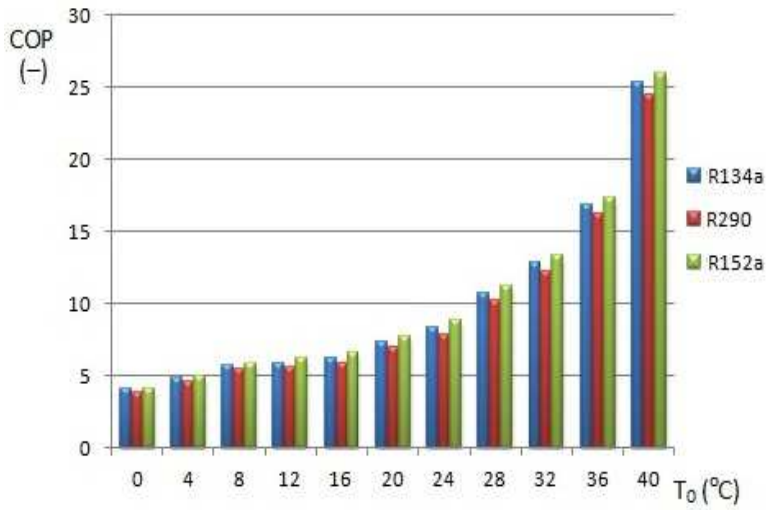

Fig. 2. Influence of T_0 on COP for the cycle with superheating and no sub cooling

Increasing the evaporation temperature while keeping constant the condensation temperature, leads to improved COP values, for all the considered refrigerants. Comparison reveals that the efficiency of single stage cycle with superheating is improved when the working fluid is R152a.

5. CONCLUSIONS

Single stage vapor compression system with R134a as working fluid is one of the most commonly used in refrigeration, including marine refrigeration.

In this paper was analyzed the cycle with superheating occurring inside the cooling space and no sub cooling. A comparison was developed for R134a and its potential alternatives: R290 and R152a, in terms of COP.

Comparative analysis is justified by possible future substitution of R134a, under Kyoto Protocol, because of its high global warming.

Properties of R152a are close to the ones of R134a; also COP values are better.

Even if R152a is a HFC like R134a, its GWP is considerable low. The best GWP is shown by R290, which is a HC, but the performance of the refrigeration system is under the one encountered for R134a.

REFERENCES

[1]. Baskaran A., Mathews Koshy P. – ***A performance comparison of vapour compression refrigeration system using eco-friendly refrigerants of low global warming potential,*** Int. Journal of Scientific and Research Publications, Vol.2, Issue 9, Sept. 2012

[2]. Harbach J.A. – ***Marine refrigeration and air-conditioning,*** *Cornell Maritime Press, pp.385, 2005*

[3]. IPCC / TEAP, 2005 – ***IPCC / TEAP Special Report: Safeguarding the Ozone Layer and the Global Climate System: issues Related to Hydrofluorocarbons and Perfluorocarbons, Chapter 4,*** Cambridge University Press, UK, pp.478, 2005

[4]. Kilicarslan A., Kurtbaş I. – ***Comparison of superheating effect of water as a refrigerant with the other refrigerants,*** J. of Thermal Science and Technology, 31, 2, pp.33-40, 2011

[5]. Paroche K., Gupta R.C. – ***Performance analysis of reciprocating compressor using eco-friendly refrigerants,*** Int. Journal of Mechanical, Automobile and Production Engineering, Vol. 2, No.9, pp.320-329, November, 2012

THE ASSESSMENT OF CONVECTIVE COEFFICIENT OF HEAT TRANSFER IN EVAPORATORS WORKING WITH R 134a, USING KANDIKLAR EQUATIONS

MITU DANIELA - ELENA

Constanta Maritime University,Romania

Heat transfer devices play important roles in the improvement of refrigeration systems performance and for this reason their design is a challenge for engineers. This paper deals with the assessment of convective coefficient of heat transfer in evaporators from one stage vapor compression systems working with R 134a, using Kandiklar equations. The general simple equations for heat exchanger analysis are introduced inside tube refrigeration evaporation where heat transfer correlations for thermal design are given. The sizing methodology of these type of heat exchangers are briefly discussed and a thermal design exemple is presented. The heat exchanger design provides missing information based on experiences, judgment and the requirements of the customer.

***Keywords**:* Kandlikar correlation, R134a, design heat exchanger

1. INTRDUCTION

Refrigerant R134a is frecquentely used in vapor compression systems on board the ships due to the fact that it has close thermodynamic properties to R12 (the traditional refrigerant for old ships) and a shows null ODP (Ozone Depletion Potential) (Memet, 2013)

In the vapor compression refrigeration system works a refrigerant in liquid state as a medium able to absorb and to eliminate heat from a space needed to be cooled.

This system contains four main components: a compressor, a condenser, an expansion valve and an evaporator, as seen in Figure 1.

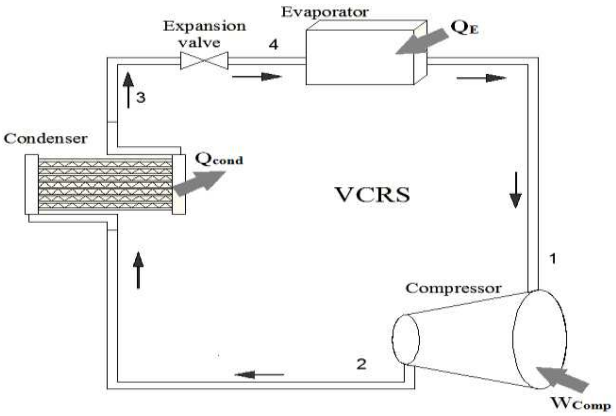

Fig. 1. Vapor compression refrigeration system

The refrigerant being in saturated vapor state enters in the compressor where it is compressed in order to reach a higher pressure and a higher temperature. Resulted vapors are led to the condenser where are cooled and condensed, while the refrigerant rejects heat to the sea water.

In the following, the refrigerant in liquid state (saturated liquid) is passed through the expansion valve, for a reduction in pressure. The resulted cold mixture is directed to the evaporator. The temperature of air from the cooled space is decreased by the evaporation of the liquid part from the cold refrigerant mixture. The refrigerant in vapor state at evaporator exit is in saturated state again. These vapors will be led to be compressed and follows other cycle.

One stage vapour compression refrigeration system presents a low side pressure, which is the pressure from evaporator and a high side pressure, meaning the pressure from the other heat exchanger- the condenser. The performance of such systems indicates that these systems are adequate as long as the temperature difference between evaporator and condenser (*temperature lift*) is small. Still, there are several applications where the temperature lift can be high enough. The temperature lift might be important either due to the requirement of very low evaporator temperatures and/or due to the requirement of very high condensing temperatures (Memet, 2012). Heat transfer devices play important roles in the improvement of refrigeration systems performance and for this reason their design is a challenge for engineers.

This paper deals with the assessment of convective coefficient of heat transfer in evaporators from one stage vapor compression systems working with R 134a, using Kandiklar equations.

2. EVAPORATORS AND CONDENSERS

Low pressure liquid leaves the metering device and enters the evaporator.

The cooler refrigerant in the evaporator tubes, absorb the heat. The change of temperature causes the refrigerant to “flash” or “boil”, and changes from a low pressure liquid to a low pressure cold vapor.

The low pressure vapor is pulled into the compressor and the cycle starts over.

The hot vapor enters the condenser and starts to flow through the tubes.

Cool air is blown across the out side of finned tubes of the condenser; usually by a fan or water with a pump.

Since the air is cooler than the refrigerant, heat jumps from the tubing to the cooler air. The energy goes from hot to cold is called latent heat.

As the heat is removed from the refrigerant, it reaches it’s saturated temperature and starts to flash (change states), into a high pressure liquid.

The high pressure liquid leaves the condenser through the liquid line and travels to the metering device.

The brazed plate heat exchanger is the most compact heat exchanger on the market today. Its high heat transfer efficiency in combination with its compact design equals a compact heat exchanger for a wide range of heating, cooling, evaporating and condensing duties. The brazed heat exchanger consist of thin corrugated stainless steel plates brazed together with copper to from a self-contained unit. Brazing the plates together eliminates the need for a frame, gaskets, bolts and the carrying bar. The result is a heat exchanger that costs less, weighs less, holds less refrigerant and takes up less space.

Shell and tube heat exchangers have been around for a long time but still offer many benefits over alternative heat exchangers. Its durability and versatility, with a wide range of material choices give the heat exchanger many advantages to meet application needs.

Shell and tube heat evaporators have larger passages, which give the unit the capability to handle dirty fluids, and also have the ability to be flushed for onsite cleaning. It can also be easily repaired, by tube plugging, tube replacement, heat replacement, without the need to replace the entire unit.

The shell side of the condenser prvides additional pumpdown capacity with the internal shell fluid inventory. Its larger passages also offer a grater control in fluid pressure drop that can be optimized when used with viscous liquids and/or high flow rate conditions. The waterside of the condenser can easily be cleaned to ensure many years of consistent performance.

Sizing the Right Evaporator: There are three basic selection methods you can use to size a evaporator. The first and easiest is to size by nominal system tons. The second method is to use compressor capacity. The third and recommended method is sizing by range, flow and approach.

Sizing a Condenser: A properly sized condenser will have a heat transfer rate equal to the system cooling load plus the energy added to the refrigerant during the compression process.

3. HEAT TRANSFER – THERMAL ANALYSIS

3.1 HEAT EXCHANGER DESIGN METODOLOGY

In Figure 2 it is shown the flow chart of heat exchanger design methodology. The first criterion that a heat exchanger should satisfy is the fulfillment of the process requirements(Kakac,1998).

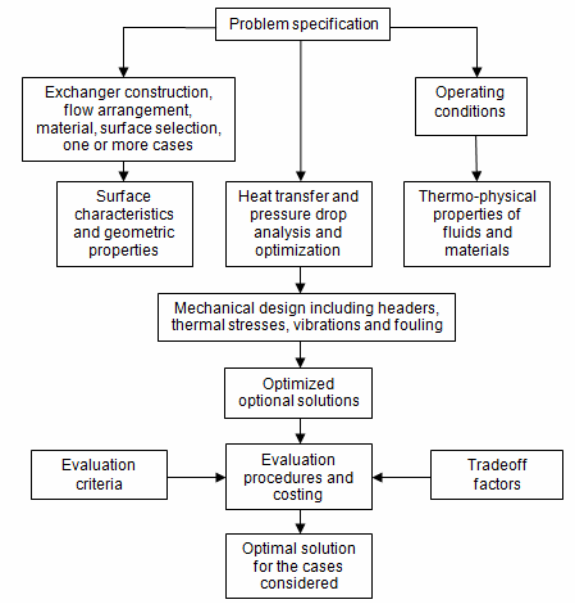

Fig. 2. Heat exchanger design metodology

The design specifications may contain all the necessary detailed information on flow rates of steams, operating pressures, pressure drop limitation for both streams, temperatures, size, length, and other design constraints such as cost, type of materials, heat exchanger type and arrangements. The heat exchanger design provides missing information based on experiences, judgment and the requirements of the customer.

The exchanger construction type, flow arrangement, surface or core geometry and materials must be selected, based on the problem specification. In the selection of the type of heat exchanger, must be considered the operating pressure and temperature levels, maintenance requirements, reability, safety, availability and manufacturability of surface and cost.

Rating is the computational process by which one determines the thermal performance and pressure drops for two streams in a completely defined heat exchanger. In the rating problem, the heat exchanger already exists or the heat exchanger configuration is selected by approximate sizing. Inputs to the rating problem are: heat exchanger surface geometry and dimensions, fluid flow rates, inlet temperatures, pressure drop limitations. The fluid outlet temperatures, total heat transferred, pressure drop for both streams through the heat exchanger are to be calculated in the rating analysis.

The selection criteria is that the heat exchanger must withstand the service conditions of the plant environment. After thermal analysis, the mechanical design is carried out which include the calculation of plate, tube, shell, header thickness and arrangements. The heat exchanger must resist corrosion by the service and process streams and by the environment.

Thermal stress calculations must be performed under steady-state and transit operating conditions. The additional important factors that should be considered and checked in the design are: flow vibrations, the level of velocities to eliminate or minimizing fouling and erosion.

After the mechanical design is completed, the firs cost analysis to arrive at an optimum solusion must be considered. An overall optimum design is the one that meets the performance requirements at a minimum cost which includes the costs of materilas, manufacturing, testing, shipment and installation and operating and maintenance costs, like: costs of fluid pumping powers, repair and cleaning.

The problem of heat exchanger design is very intricate. Because of a large number of qualitative judgements, trade-offs and compromises, heat exchanger design is more of an art than a science at this stage.

3.2. HEAT TRANSFER EQUATIONS

In this section is given an overview of general heat exchanger analysis and design techniques along with special considerations required for refrigeration and air-conditioning application.

In the heat transfer applications, the overall heat transfer coefficient is usually based on the cold side or hot side area and it is obtained by combining thermal resistances as:

$$\frac{1}{U_o} = \frac{A_o}{A_i}\frac{1}{\eta_i h_i} + \frac{A_o}{\eta_o}\frac{R_{fi}}{A_i} + A_o R_w + \frac{R_{fo}}{\eta_o} + \frac{1}{\eta_o A_o} \tag{1}$$

where: A_o - the total outside area, $A_o = \pi d_o N_t L$;

η - the overall surface efficiency, $\eta = \left[1-\left(1-\eta_f\right)\frac{A_f}{A}\right]$;

R_{fi}, R_{fo} - inside and outside foulig factors.

On the right hand side of equation (1) the terms represents inside convective resistance, inside fouling resistance, wall resistance, outside fouling resistance and outside convective resistance respectively.

The heat transfer rate can be obtained from the following basic equation:

$$Q_r = \dot{m}_r\left(i_o - i_i\right) \tag{2}$$

$$Q_f = \dot{m}c_p\left(T_{fo} - T_{fi}\right) \tag{3}$$

$$Q = U_o A_o \Delta T_m \tag{4}$$

where: ΔT_m is defined as the log-mean temperature difference as:

$$\Delta T_m = \frac{\Delta T_1 - \Delta T_2}{\ln\left(\frac{\Delta T_1}{\Delta T_2}\right)} \tag{5}$$

$\Delta T_1, \Delta T_2$ - the local temperature differences for the refrigerant and the fluid at the inlet and outlet of the heat exchanger respectively.

For the local analysis, the equations are solved over incremental heat exchanger lengths from one end of the heat exchanger to the other end. The heat transfer rates for each increment are then integrated over the heat exchanger to obtain the total heat transfer. The complicating factor in refrigeration and air conditioning heat exchangers, is that the refrigerant is not two phase over all its length.

The size of the heat transfer exchanger can be obtained from equation (4).

The overall heat transfer coefficient, U_o, based on the outside diameter of tubes can be estimated from the estimated values of individual heat transfer coefficients, wall and fouling resistance and the overall surface efficiency using equation (1).

Heat load can be estimated from:

$$Q = \left(\dot{m}c_p\right)_c\left(T_{c2} - T_{c1}\right) = \left(\dot{m}c_p\right)_h\left(T_{h1} - T_{h2}\right) \tag{6}$$

If one stream changes phase:

$$Q = mi_{fg} \tag{7}$$

where: m – the mass of the stream changing phase per unit time

i_{fg} - the latent heat of the phase change.

After ΔT_m is calculated, the objective is to find the right number of tubes of diameter, d_o, and the shell diameter, D_s, to accommodate the number of tubes, N_t, with given tube length, L.

The total number of the tubes, N_t, can be predicted in fair approximation as function of the shell diameter by taking the shell circle and dividing it by the projected area of tube layout pertaining to a single tube A_1:

$$N_t = (CTP)\frac{\pi D_s^2}{4A_1} \tag{8}$$

where: CTP – the tube count calculation constant, which accounts for the incomplete coverage of the shell diameter by the tubes, due the necessary clearances between the shell and the outer tuber circle and tube omissions due to tubes pass lanes for multi-tube pass design.

3.3. KANDLIKAR CORRELATION

Kandlikar derived a correlation for flow boiling of pure liquids in smooth tubes (Kandlikar,1990). It was developed by using an extensive data bank of over 10,000 data points with water, refrigerants and cryogens. This correlation was able to represent the trends in *h* versus quality *x*, mass flux *G*, and heat flux *q"*. Kandlikar suggested modifications by incorporating other correlations for calculating the single phase heat transfer coefficient with all flow liquid, h_{Lo} (Kandlikar,1991). The flow boiling correlation for pure liquids is as follows:

$$h_{TP} = \text{larger} \quad \text{of} \begin{cases} h_{TP,NBD} \\ h_{TP,CBD} \end{cases} \tag{9}$$

where: NBD – nucleate boiling dominant region
CBD – convective boiling dominant region.

$$h_{TP,NBD} = 0{,}6683Co^{-0,2}(1-x)^{0,8}h_{LO} + 1058Bo^{0,7}(1-x)^{0,8}F_{fl}h_{LO} \tag{10}$$

$$h_{TP,CBD} = 1{,}136Co^{-0,9}(1-x)^{0,8}h_{LO} + 667{,}2Bo^{0,7}(1-x)^{0,8}F_{fl}h_{LO} \tag{11}$$

For horizontal tubes with Froude number, Fr_{LO}, defined as $Fr_{LO} = \frac{G^2}{\rho_l^2 gd}$, less than 0,04, a multiplier $(25Fr_{LO})^{0,324}$ is applied to the first terms in equations (9) and (10). For $Fr_{LO} > 0{,}04$, and for vertical tubes no correlation is needed. This correction is usually not needed for the range of mass fluxes employed in the refrigerant evaporators. *Bo* is the boiling number, $Bo = \frac{g''}{Gh_{fg}}$. *Co* is the convection number given by $Co = (\rho_v / \rho_l)^{0,5}[(1-x)/x]^{0,8}$.

F_{fl} is fluid-surface parameter related to the nucleation characteristics. For R134a, $F_{fl} = 1{,}63$. h_{Lo} is the single-phase heat transfer coefficient.

For $0{,}5 \le \mathrm{Pr_l} \le 2000$ and $10000 \le \mathrm{Re_{LO}} \le 5000000$:

$$Nu_{LO} = h_{LO} D / k_l = \mathrm{Re}_{LO}\, \mathrm{Pr}_l (f/2) / \left[1{,}07 + 12{,}7 \cdot \left(\mathrm{Pr}_l^{2/3} - 1\right)(f/2)^{0{,}5}\right] \quad (12)$$

For $0{,}5 \le \mathrm{Pr_l} \le 2000$ and $2300 \le \mathrm{Re_{LO}} \le 10000$:

$$\mathrm{Nu_{LO}} = \mathrm{h_{LO}} D / \mathrm{k_l} = (\mathrm{Re_{LO}} - 1000)\, \mathrm{Pr_l} (\mathrm{f}/2) / \left[1 + 12{,}7 \cdot \left(\mathrm{Pr_l}^{2/3} - 1\right)(\mathrm{f}/2)^{0{,}5}\right] \quad (13)$$

The friction factor *f* in equations (12) and (13) is given by:

$$\mathrm{f} = \left[1{,}58 \ln\left(\mathrm{Re_{LO}}\right) - 3{,}28\right]^{-2} \quad (14)$$

4. RESULTS

In this paper, in the assessment of convective coefficient of heat transfer in evaporators from one stage vapor compression systems was used as refrigerant R134a.

The working conditions was:

- circular tube diameter = 8 mm;
- tube length = 5 m;
- mass flux = 100 kg/m^{2}s;
- temperature = -5^{o}C;
- heat flux = 10 kW/m^2.

As results, in the next figures it is presented the influence of quality on heat transfer coefficient and influence of mass flux on heat transfer coefficient.

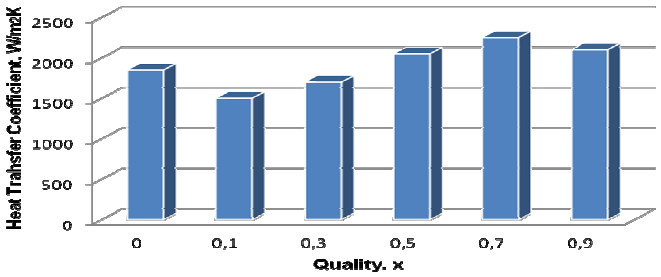

Fig. 3. The influence of quality on heat transfer coefficient inside tube flow of R134a

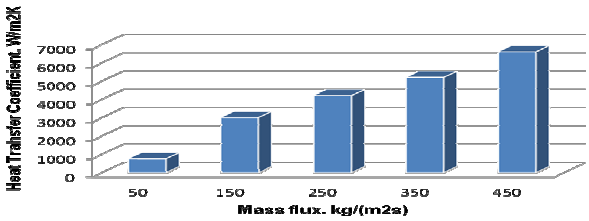

Fig. 4. The influence of mass flux on heat transfer coefficient inside tube flow of R134a

5. CONCLUSIONS

The thermal design methods of evaporators from one stage vapor compression systems are the same as single phase applications or as power and process industries. The only difference will be in the selection of proper correlations to calculate heat transfer coefficients on the refrigerant side. The correlations given to calculate heat transfer coefficient for refrigerant are often different from other fluids in that they are derived from a refrigerant database.

The convective coefficient of heat transfer in evaporators from one stage vapor compression systems working with R134a was analyzes considering the vapor quality and the mass flux. The entering quality is 0,0 and the existing qulity is 0,9. Taken into account the working conditions and using the Kandlikar correlation, was determined the variation of evaporation heat transfer, h_{TP}, as a function of vapor quality, *x*. In this way, was obtained for $x = 0{,}1$ the minimum value of heat transfer coefficient, $1800W/m^2K$, and for $x = 0{,}7$, the maximum value of heat transfer coefficient, $2200W/m^2K$.

Then was determined the variation of evaporation heat transfer inside the tube flow of R134a, h_{TP}, as a function of mass flux. For mass flux $50kg/m^2s$, $h_{TP} = 500W/m^2K$, and for mass flux $450kg/m^2s$, $h_{TP} = 6200W/m^2K$. Can be noticed an exponential increase of heat transfer coefficient with mass flux.

The Kandlikar correlation was able to predict the correct trends for refrigerants and water. The correlation was recently extended to compact evaporators, microfin tubes and binary mixture as well.

REFERENCES

[1]. Kakac, S. – ***Evaporators and condensers for refrigeration and air conditioning systems and their thermal desin***, International Mechanical Instalation Science & Technology Symposium'98, pp. 109-168, 1998.

[2]. Kandlikar, S.G. – ***A general correlation for saturated two-phase flow boiling heat transfer inside horizontal and vertical tubes***, Journal Heat Transfer, Vol. 11, pp. 219-228, 1990.

[3]. Kandlikar, S.G. – ***Development of A Flow Boiling Map for Subcooled and Saturated Flow Boiling of Different Fluids in Circular Tubes***, In Heat Transfer with Phase Change, Habib, IS. Et al., eds, ASME HTD, Vol. 114, pp. 51-62, 1990. Also published in Transactions of ASME, Journal of Heat Transfer, Vol. 113, pp. 190-200, 1991.

[4]. Memet, F.- ***A first and second law analysis developed on a two stage vapour compression refrigeration system***, Journal of Marine Technology and Environment, pp 81-86, Vol I, 2012

[5]. Memet, F. – ***A theoretical analysis of a vapour compression system on environmental and thermodynamic basis,*** Journal of Marine Technology and Environment, pp 33-40, Vol II, 2013

THE ANALYSIS OF SHORT-CIRCUIT CURRENTS IN A NAVAL ELECTRICAL NETWORK BY MEANS OF SOFTWARE TOOLS

[1]SAMOILESCU GHEORGHE, [2]MARIN GEORGIANA

[1]*"Mircea cel Batran" Naval Academy,* [2]*Reseach Center for Navy, Romania*

Short circuits in naval electrical networks are complex phenomena affecting all electrical equipment due to the short length of circuits. The calculation of short circuit currents and their taking into account, ranging from design to the operation of naval equipment and installations, ensure the equipment reliability and optimization. Based on industry standard data, the paper analyzes the management of a particular ship power system, by performing the short-circuit current calculation based on a software tool, particularly designed for this purpose.

Keywords*:* Naval electrical network, Short circuit current, Software tool

1. INTRODUCTION

The availability of electricity on board ships is ensured by the equipment therein, given by the existence of an onboard electric power plant capable of generating the necessary energy to support the entire load [2, 3, 9, 10].

Short circuits in naval electrical networks are complex phenomena affecting all electrical equipment onboard, and are influenced by the particularities of the naval electrical network [3, 4, 11]. The short circuit analysis of such a network, imposed by IEC 61363-1, is complex and time consuming. Therefore, a software tool was developed on particular case – a container carrier ship of 35000 tdw. The results were compared to the available data regarding that particular ship, providing an efficient and accurate solution. The software program, developed in Visual Basic, allows the parameters adjustment of the electrical installations and could be extended to suit other electrical networks.

2. THE SHORT CIRCUIT CURRENTS ISSUES IN NAVAL ELECTRICAL NETWORKS

In order to quantify the possible effects of short circuit currents in electrical installations and to determine the measures for ensuring damage protection, the design of electrical devices must include the specification of several quantities that define the short circuit currents [4, 11]. The main medium voltage distribution network is mainly comprised of a three-phase system, of three conductors without neutral [2, 10]. The knowledge of short circuit current values enables solutions to some serious design and exploitation issues.

Short circuit currents are affected by several naval electrical installations particularities, including:

- low nominal voltages and high powers of synchronous generators;
- high short circuit and nominal currents;
- low impedance circuits due to short current paths;
- higher circuit resistance compared to corresponding reactance;
- large variations in generating power in various operating regimes and accordingly large variations in short circuit currents compared to the initial operating regime;
- high inequalities between time constants of paralleled synchronous generators excitation coils [10].

The points of computing short circuit currents are thus chosen so that currents passing through the tested devices reach maximum values.

The instantaneous value of the short circuit current is comprised of:

- the instantaneous periodic component – the imposed current (i_p) and
- the instantaneous non-periodic component – the free current (i_a) [2].

$$i = i_p + i_a \tag{1}$$

The instantaneous short circuit current value and its components are computed based on the relation:

$$i(t) = \frac{E_m}{Z}\sin(\omega t + \alpha - \varphi) - \frac{E_m}{Z}\sin(\alpha - \varphi)\cdot e^{-t/T_a} \tag{2}$$

Here E_m represents the amplitude of the electromotive force, considered constant during the short circuit:

$$e = E_m \cdot \sin(\omega t + \alpha) \tag{3}$$

Here α represents the initial phase, Z is the impedance module, and φ is the impedance argument. There are denoted: X - the circuit reactance, R – the circuit resistance, and L – the inductance. The constant T_a represents the damping constant of the non-periodic component of the short circuit current.

The short circuit current shock represents the highest instantaneous value of the total short circuit current, corresponding to the initial half of the first period. The period denoted with T, is the inverse of the frequency f. Assuming constant the periodic component of the short circuit current, the shock current becomes:

$$i_{soc} = I_{m0}\cdot\left(1 + e^{-\frac{R}{2fL}}\right) \tag{4}$$

Here, I_{m0} represents the initial value of the periodic component amplitude, and f is the frequency.

The analytical method of computation of short circuit currents is based on the equivalent generator nominal quantities [4]. The equivalent generator represents all generators working in parallel. The basic quantities of the equivalent synchronous generator are the base power, voltage, current, and impedance. The base power is computed as the sum of all parallel generators nominal power.

$$S_b = \sum_{i=1}^{n} S_{nom\,i} \quad [kVA] \tag{5}$$

The base voltage U_b equals the nominal line voltage U_{nom} of the generators, whereas the base current I_b represents the sum of all parallel generators nominal currents.

$$I_b = \sum_{i=1}^{n} I_{nom\,i} = \frac{S_b}{U_b\sqrt{3}} \quad [kA] \tag{6}$$

Finally, the base impedance of the equivalent generator is:

$$Z_b = \frac{U_b}{I_b\sqrt{3}} \quad [m\Omega] \tag{7}$$

The calculation of short circuit currents employs the relative quantities, expressed as the ratio between the absolute physical quantity A and the base quantity A_b. In this case, the measurement unit of the relative quantity is the percentage unit p.u.

$$a = \frac{A}{A_b} \tag{8}$$

In order to determine the short circuit currents a schematic diagram is established [11], including all elements concurring to the short circuit current assessment and the circuit components to be tested for electro-dynamical and thermal stability – generators, transformers, switches, cables, bars, etc.

The analytical method of computing the short circuit currents relies on the use of all equations describing the short circuit processes in electrical machines and networks [2, 4].

Due to calculus complexity, the method implementation is difficult; therefore computing machines are involved to eliminate calculus difficulties [12]. Employing a particular software tool for this purpose diminishes the computation time, increases accuracy and determines the time variation of all measures describing the short circuit. It also allows the assessment of the impact of various factors affecting the short circuit process.

There are several standards regarding the issue of short circuit currents in various power plants, electrical devices and electrical networks [13–17].

The IEC 61363-1 and SR/CEI/60092 standards refer to electrical equipment onboard ships and marine structures [13, 15]. The computing procedures relate to symmetrical three-phase short circuits or phase-to-hull short circuits, in which the short circuit emerges simultaneously for the three poles.

Asymmetrical short circuits can lead to high values of non-periodic short circuit currents, to which the supply cables impedance should be added.

Phase-to-phase short circuits in three-phase networks generally turn into three-phase short circuits because the flaming arcs of phase-to-phase short circuits burn the phase insulation. The short circuit depends upon various factors: the time and place of short circuit, the number of grounding points, etc.

The IEC 60909 standard refers to short circuit currents in three phase AC systems and currents generated from two simultaneous line-to-earth short circuits, to which partial short circuit currents flowing to the ground are added [14]. The standards establish calculation procedures related to line-to-earth short circuits, produced in solidly earthed neutral systems or impedance earthed neutral systems. These apply to short circuits in three-phase AC systems operating at 50 or 60 Hz nominal frequency.

3. THE MARINE ELECTRICAL NETWORK PARAMETERS

The short current analysis was performed on the electrical network of a container carrier of 35000 tdw [1, 18, 19], with a power supply group comprised of three 2200 kW and two 2800 kW diesel generators, and one emergency generator if 500 kW. The ship has two main engines of 18300 kW and one 2500 kW bow thruster.

There was employed the simplified diagram of the medium voltage distribution system, comprised of:

- two 2800 kW diesel generators,
- three 2200 kW diesel generators,
- power distribution systems and
- various elements such as: transformers, circuit breakers, cables.

The main parameters, representing the input data for the generators and main engines are described in Tables 1 and 2. These parameters range from power, voltage, current, frequency, and power factor, to stator resistance, reactance, and parameters of the afferent cable.

Table 1: Synchronous Generators And Afferent Cables Input Parameters

Synchronous generator	Meaurement unit	Generator 2800 kW	Generator 2200 kW
Apparent power	kVA	3733.33	2933.33
Voltage	V	6600	6600
Frequency	Hz	60	60
Current	A	326.6	256.6
Power factor cos φ		0.75	0.75
Stator resistance Ra	p.u.	0.8	0.82
Sub-transient reactance (d-axis) X''d	p.u.	13.8	14.3
Transient reactance (d-axis) X'd	p.u.	24.7	25.2
Reactance(d-axis) Xd	p.u.	245	245
Sub-transient time constant T''d	ms	6.3	6.5
Transient time constant T'd	ms	248.4	257
D.C. time constant Tdc	ms	44	45.1
Cable - Number of cables N		2	2
Resistance R	Ω/km	0.195	0.27
Reactance X	Ω/km	0.117	0.122
Length of cable L	m	30	30

Table 2: Main Engines And Afferent Cables Input Parameters

Engine	Meaurement unit	Bow thruster engine	Pump engine
Power	kW	2500	355
Voltage	V	6600	6600
Current	A	280.7	37.6
Power factor cos φ		0.82	0.87
Rotor resistance Rr	p.u.	2.98	1.58
Stator resistance Ra	p.u.	0.77	0.69
Sub-transient reactance X''m	p.u.	15.33	11.93
Cable - Number of cables N		2	1
Resistance R	Ω/km	0.27	1.16
Reactance X	Ω/km	0.122	0.152
Length of cable L	m	300	80

4. DESCRIPTION OF THE COMPUTATION METHOD AND SOFTWARE TOOL

The short circuit current calculation was performed in various network points, in order to determine whether the system components are able to withstand short circuit and to select the appropriate protection equipment. The calculation method was based on the IEC 61363-1 standard [4, 11 - 13].

In the scope of facilitating the short circuit computation, and concurrently maintaining high computation accuracy, the analytical method using all equations that describe the short circuit processes occurring in electrical machines and networks was implemented through a software tool custom-built for the analyzed electrical network, in the Visual Basic programming language [7].

Based on the simplified electrical scheme of the 6600V AC distribution system, illustrated in Fig. 1, the impedance of every circuit part is computed [4, 11, 19]. Herein, there is also represented one example location of the short circuit occurrence – the medium voltage switchboard bus.

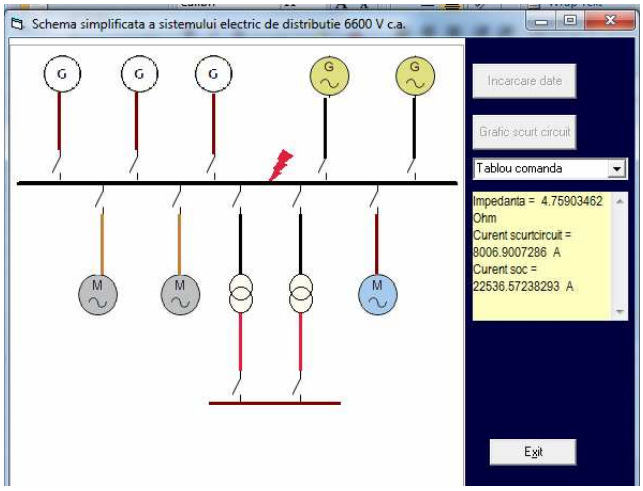

Fig. 1. Schematic diagram of the ship medium voltage distribution system and the selection of the short circuit occurrence point

The equivalent generator theorem [2] was applied for the first part; according to it, several generators working in parallel mode on the same vertex may be replaced by a single generator with equivalent electromotive force and impedance - E_{ech} and Z_{ech_g}, respectively.

The first step in computing the short circuit current consists in determining the equivalent impedance of the upstream circuit relative to the short circuit occurrence point. The equivalent resistance and reactance of two generators working in parallel are computed with the relations:

$$R_{aech} = \frac{R_2\left(R_1^2 + X''^2_1\right) + R_1\left(R_2^2 + X''^2_2\right)}{\left(R_1 + R_2\right)^2 + \left(X''_1 + X''_2\right)^2} \tag{9}$$

$$X''_{dech} = \frac{X''_2\left(R_1^2 + X''^2_1\right) + X''_1\left(R_2^2 + X''^2_2\right)}{\left(R_1 + R_2\right)^2 + \left(X''_1 + X''_2\right)^2} \tag{10}$$

The resistance is computed as summation of stator resistance and line resistance, while the reactance is the sum between the direct axis (d-axis) sub-transient reactance and line reactance.

For each circuit element in the simplified electrical network, there is available a set of data representing the main parameters. Moreover, the software tool provides the user a particular menu for the configuration of the respective parameters. After the data for the entire electrical scheme has been loaded, the option of computing the short circuit current in several predetermined locations becomes available. The short circuit occurrence points list consists in several relevant computing points, such as the 6600 V AC distribution system main panel terminal, the generator terminals, or the main electrical engines terminals.

The location of the short circuit being selected, we can proceed to the calculation of the short circuit current. The software identifies each element in the electrical scheme and its parameters, then performs the calculation of the equivalent impedance of the entire portion of the circuit located upstream of the short circuit occurrence point.

Since the short circuit current represents the sum of two components, there are computed both the periodic and non-periodic component, as well as their sum, with the relations below, where I_{sc} is the amplitude of the short circuit current.

$$i_p(t) = I_{sc} * \sqrt{2} * \sin\left(2\pi * f * t + \frac{\pi}{4} - arctg\left(\frac{X_{ech}}{R_{ech}}\right)\right) \tag{11}$$

$$i_a(t) = -I_{sc} * \sqrt{2} * \sin\left(\frac{\pi}{4} - arctg\left(\frac{X_{ech}}{R_{ech}}\right)\right) * e^{-\frac{2\pi * f * t}{X/R}} \tag{12}$$

5. THE RESULTS

Table 3 describes the short circuit current components value computed in the case of short circuit at the main distribution panel and at the bow thrusters engine, for the moments of time t = 0.5*T, and t = 5*T.

Table 3: Short circuit currents at relevant points on the electrical distribution network

	Main distribution panel		**Bow thruster engine 2500 kW**	
	t = 0.5*T	**t = 5*T**	**t = 0.5*T**	**t = 5*T**
Periodic component $i_p(t)$ [A]	8924.05	8924.05	43173.05	35319.75
Non-periodic component $i_a(t)$ [A]	142.89	0	0.12	0
Total current i(t) [A]	9066.94	8924.05	43173.17	35319.75

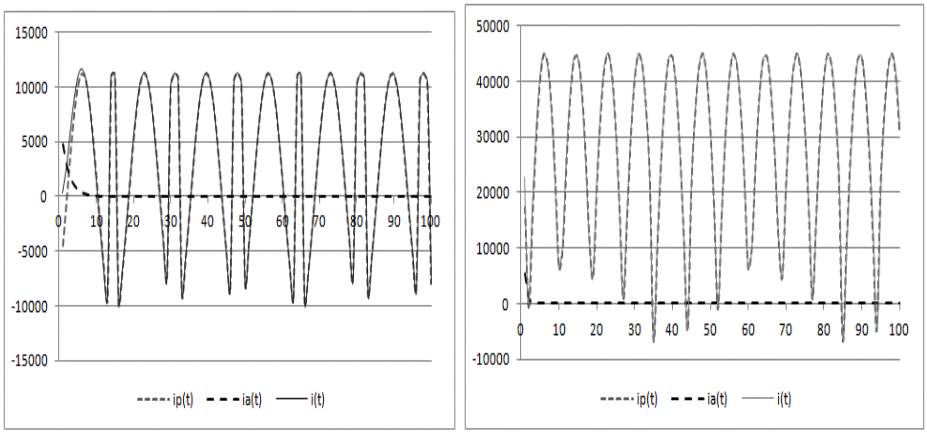

Fig. 2. The short circuit currents at the main distribution panel (left) and at the bow thruster engine (right)

Fig. 2 illustrates the short circuit current components variation in time with the step of 1 millisecond, as represented by the software tool. The chart on the left side illustrates the short circuit currents computed at the main distribution panel, whereas the chart on the right side describes the variation of the short circuit currents computed at the bow thrusters engine. Both charts are represented for the time range of 100 milliseconds, from the moment of the short circuit occurrence.

6. RESULTS DISCUSSION

Fig. 2 describes the variation of both periodic and non-periodic components of the short circuit current, as well as their sum, in the case of the a short circuit occurrence at the main distribution panel and at the terminals of an essential electric engine – the bow thruster engine, of 2500 kW.

The periodic component, computed with relation (11), and represented with a grey dotted line, has an approximate sine variation and lasts throughout the entire time range. The non-periodic component, illustrated with a black dashed line and computed with relation (12), lasts for 46 milliseconds and 14 milliseconds, respectively. Its value at t=0 depends upon the initial total short circuit current value.

Due to the non-periodic component, the total short circuit current, represented with a continuous line, exceeds the instantaneous value of the periodic component for the first half of period. After the non-periodic component fades out, the total short circuit current identifies with its periodic component.

The values in Table 3 are given for the first half period t= 0.5*T, representing the shock current (4), and for t = 5*T, of approximately 83 seconds.

The results are close to the available data on the ship electrical network, stating that the short circuit currents for the first half period are of the order of magnitude of a few tens of thousands of Ampers, decreasing to several thousands of Ampers after five periods t = 5*T.

The software program computes the short circuit currents variation for the selected occurrence point and in the case of all generators operating condition, thus providing a complete description of the respective currents. It also renders the possibility of modifying the parameters of the elements of the electrical network, or selecting various relevant points of short circuit occurrence. The software program could be extended such as to apply to various ship electrical networks.

7. CONCLUSIONS

The calculation of short circuit currents is performed in order to establish whether the system components have the ability to withstand short circuit and to enable the appropriate selection of protection equipments, as method of optimization of the ship electrical network [5, 6, 8].

Hence there was performed the short circuit currents analysis within the electrical network of a particular ship, optimized through the implementation of an algorithm within a software application. The algorithm is based on the IEC 61363 standard. The computing procedures of three-phase AC symmetrical short circuit currents are thereby applied, irrespective of the asymmetrical short circuit conditions. The results are close to the scarce data available for that particular ship.

The software program would be rendering a time efficient tool in the analysis of the marine electrical networks, in order to determine the equipment characteristics to withstand the appropriate loads.

REFERENCES

[1]. Ådnanes K. – ***Maritime Electrical Installations And Diesel Electric Propulsion***, ABB AS Marine, Oslo, Norway, 2003

[2]. Călueanu D. et al. - ***Shipboard electrical installations*** (in Romanian), Technical Publishing House, Bucharest, 1981

[3]. Czarkowski D. - ***Ships' electrical power network systems protected from damages caused by short-circuit current other than three-phase symmetrical current***, "Aeronautics and surface transport days" Conference, Warsaw, Poland, 2005

[4]. de Metz-Noblat B. et al. - ***Calculation of short-circuit currents*** (Cahier technique no. 158), Schneider Electric, 2005

[5]. Radan D. - ***Power/Energy Management Of Marine Power Systems*** (Technical Report), NTNU, Trodtheim, Norway, 2004

[6]. Radosavljevic J., Klimenta D., Jevtic M. - ***A genetic algorithm-based approach for a general steady-state analysis of three-phase self-excited induction generator***, Rev. Roum. Sci. Techn. – Électrotechn. et Énerg., 57, 1., pp. 10–19, 2012

[7]. Tylee L. - ***Learn Visual Basic 6.0***, Kidware, Bellevue, Washington, pp. 100-177, 1998

[8]. Serban Gh., Ionescu L., Mazare A. - ***The possibility of optimisation for power supply consumption using evolvable power regulator***, Rev. Roum. Sci. Techn. – Électrotechn. et Énerg., 57, 2, p. 222–231, 2012

[9]. Valkeejärvi K. - ***The ship's electrical network, engine control and automation***, Koninklijk Gallois Genootschap no.3, 2006

[10]. *** - ***Electric Power Distribution Systems***, Naval Ships' Technical Manual Chapter 320, 1998

[11]. *** - ***Short-Circuit Method IEC 61363*** Technical Reference, DIgSILENT GmbH, Germany, 2009

[12].*** ***- PTW IEC_61363 Short Circuit Study***, SKM Power Tools, Data Sheet, 2011

[13]. *** - ***International Standard IEC 61363-1***, 1998

[14]. *** - ***International Standard IEC 60909*** - part 0, 2001, part 3, 2003

[15]. *** - ***Standard ST/CEI/60092*** - part 301, 302, 303, 304, 305, 350, 351, 352, 353, 354, 359, 373, 374, 375, 376, 502, 504, 2007

[16]. *** - ***Normative I 7- 2009-2***, 2009

[17]. *** - ***Directive of the European Parliament and the Council for establishing the technical requirements for interior navigation ships, 2006/87/CE***, In: Standardization Bulletin ASRO, March 2012

[18]. *** - ***Generalities on naval systems and installations on board*** (Technical Application Papers No.12), ABB SACE, Bergamo, Italy, 2011

[19]. *** - ***Basic Principles of Ship Propulsion***, MAN Diesel &Turbo, Copenhagen, Denmark, 2011.

ECOTOXICOLOGICAL ASSESSMENT IN SOME POINTS OF THE ROMANIAN BLACK SEA COASTAL ZONE

SUNDRI MIRELA – IULIANA

Constanta Maritime University, Romania

An ecotoxicological assessment on four points of the Romanian Black Sea coastal zones ecosystems was done using a 72 h algal growth inhibition microbiotest. Water samples toxicity has been tested on the *Phaeodactylum tricornutum*. Inhibition of algal growth ranged between 2% and 17%. Generally, *Phaeodactylum tricornutum* shows adaptability tendency to the specific conditions of the investigated areas during the time of the test.

***Keywords**:* Black Sea, ecotoxicological assessment, algal growth inhibition, microbiotests,

1. INTRODUCTION

The Black Sea is particularly susceptible to eutrophication due to its huge freshwater catchment coupled with the isolation from the flushing effects of the open ocean.

Despite the excessive fishing, pollution and eutrophication which generated the decline of the biological resources in the Black Sea, there are certain signs of revitalization: the algal bloom are becoming less frequent and less intense; the abundance of fodder zooplankton and the small pelagic fish is increasing (The Commision on the Protection of the Black Sea Against Pollution, 2009).

There are some specific sites in the Black Sea where are present relatively high contamination levels for some pesticides, heavy metals and PCBs. The concentrations of some substances have sometimes values above the accepted ranges used as Ecotoxicological Assessment Criteria. In this manner, toxicity tests are typically conducted to measure the effects of a substance on a living organism. These tests are essential in the monitoring of environmental pollutants. Bioassays are becoming important in ecotoxicological risk assessment of contaminated areas, including coastal zones (Persoone et al., 2003; Committee on Toxicity Testing, 2007).

Microbiotests used test species, which are independent of the sourcing, the culturing and the maintenance of live stocks of test biota.

2. METHODS

In March 2012, water samples were collected at 2 m depth from four Romanian Black Sea coastal points: Casino Mamaia (44.235722 N; 28.628858 E), Constanta “Modern Beach” (44.180258 N; 28.660465 E), Constanta “Tomis Harbor” (44.174938 N; 28.662338 E)

and Costinesti “ship wreck” (43.960578 N; 28.648460 E) areas, using a Schindler-Patalas device.

Water toxicological assessment has been made using a 72h algal growth inhibition biotest with the marine diatom *Phaeodactylum tricornutum*. For growing algal cells an incubator with 20^0C temperature controlled and a 10000 lux constant illumination has been used. The test was performed with batch PT240811, according to “Marine Algaltoxkit standard operational procedure” (Microbio Test Inc.1996).

The Algaltoxkit technology is bassed on the rapid measurement of the optical density of algal cell suspensions. Measurement of optical density was performed with a Jenway 6300 spectrophotometers and 670 nm filter, equipped with a holder for 10 cm cells. Optical density was converted into algal numbers using the characteristic equation corresponding to the batch work (sheet included in Algaltoxkit):

$y = (1685849\ x - 105857)$

(y=cells number and x=optical density)

Specific growth has been calculated with the equation:

$$\mu = (\ln N_2 - \ln N_1) / (t_2 - t_1)$$

where

t_1 time of test start;

t_2 time of test finish

N_1 initial number cell density;

N_2 cell density at t_2;

Algal growth inhibition to each sample point is calculated:

$$I_\mu = 100\ (\mu_c - \mu_t) / \mu_c\ [\%]$$

where

μ_c specific growth under the control test;

μ_c specific growth at each test sampling point.

3. RESULTS

The experiment started with the same cells number in all four samples point (10466 cells/mL). After 24h, 48h and 72h the algal cell number has been converted from optical density (Fig.1).

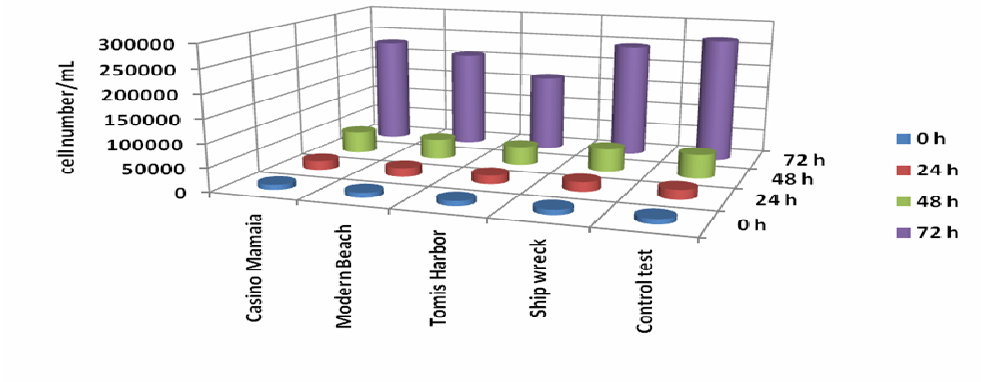

Fig.1. Algal concentration

Costinesti “Ship wreck” samples showed the highest algal cell concentration after the all three periods of growing. In this point, the *Phaeodactylum tricornutum* cell number has been 98% from the control cell concentration, after first day experiment, 96% after second day and 92% at the end of experiment (72h).

The lowest concentration of algal cells was calculated for “Tomis” Constanta Harbour: 89% from the control cell concentration after 24h, 78% after 48h and 62% after 72h, respectively. For others two samples points the algal concentration showed values between 78% and 96% from control test.

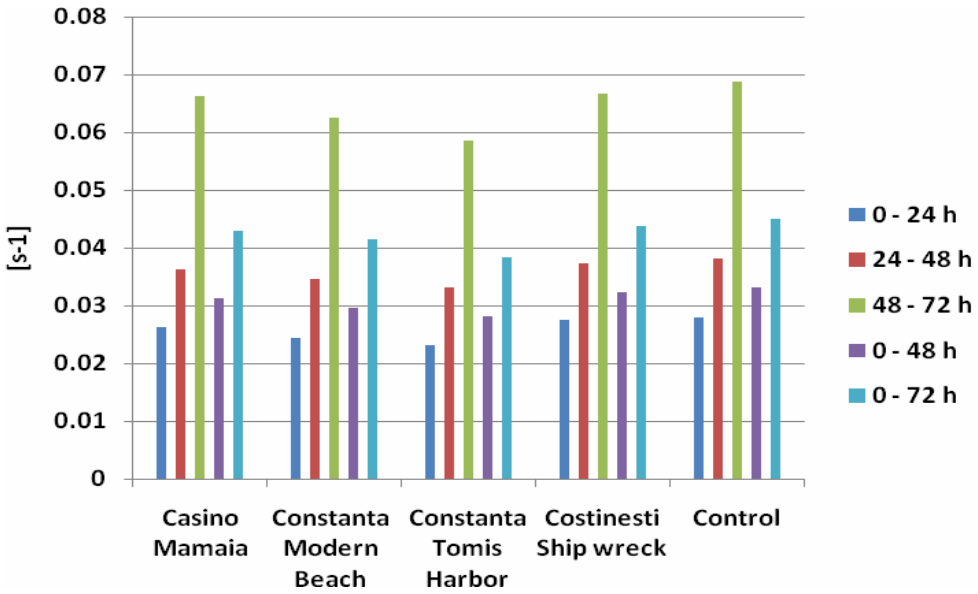

Fig.2. Algal growth rate [s-1]

Generally, from day to day, increasing trends have been observed for algal growth rates in the sample points: an average of 0.025 s^{-1} after first day has been calculated, 0.035 s^{-1} after second day and 0.063 s^{-1} after third day, respectivelly (Fig. 2). These behaviors suggest an adaptation of algal populations at the stress factor. Tomis harbor sample showed the lowest growth rate for each period of testing (82.2% ÷ 85.3% from control group growth rates).

The algal cell growth inhibition ranged between 2.2 % on Costineşti ship wreck (after 24h of experiment) and 17.8% on Tomis harbor (after 24h).

Excepting Costineşti sampling point, the cell growth inhibition decrease during the time of experiment.

The highest percentage of algal cells growth inhibition was found for Tomis Harbor water sample: 17.7% after 24h; 15.22% after 48h and 14.97% for the whole period of testing (72h). The algal growth inhibition was less then 13% for others sampling points, with an average of 5.6% for Casino Mamaia, 10.5% for „Modern” beach and 2.36% for Costineşti (Fig.3).

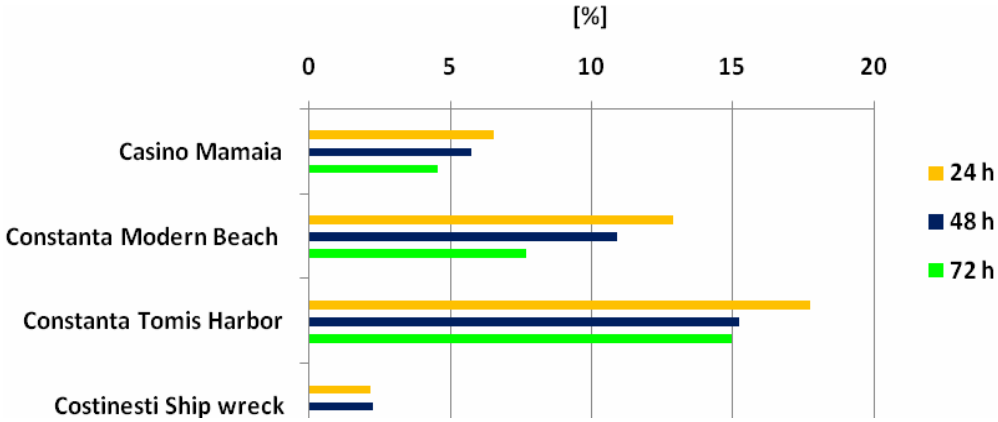

Fig. 3. Algal growth inhibition

4. CONCLUSIONS

Marine Algaltoxkit test based on the diatom *Phaeodactylum tricornutum* allowed us to highlight the following:

- Black Sea water on the sampling points has had an inhibition effect on algal growth by up to 18%, registered in Constanta Tomis harbor.
- For bathing areas (Casino Mamaia, Modern beach Constanța and Costineşti Ship wreck) the algal inhibitions not exceed 13%.
- The lowest effect of algal growth inhibition was recorded for water of the Costineşti Ship wreck.
- The effect on algal growth inhibition decreased with increasing length of the test, in all four points of the sample. This suggests a algal tendency to adapt to the specific conditions of the environment in the areas tested.

The values for algal growth inhibition, found in the water samples taken from these four Black Sea sites, does not have a significant toxicity for *Phaeodactylum tricornutum* growth.

REFERENCES

[1]. Committee on Toxicity Testing and Assessment of Environmental Agents, Board on Environmental Studies and Toxicology, Institute for Laboratory Animal Research, Division on Earth and Life Studies, National Research Council *of the National Academie.* ***Toxicity Testing in the 21st Century: A Vision and a Strategy,*** *2007.* http://www.nap.edu/catalog/11970.html

[2]. Microbio Test Inc. ***Algaltoxkit. Toxicity test with microalgae. Standard operational procedure***, 1996

[3]. Persoone, G., Marsalek, B., Blinova, I., To¨ro¨kne, A., Zarina, D., Manusadzianas, L., Nalecz-Jawecki, G., Tofan, L., Stepanova, N., Tothova, L. and Kolar, B. ***A practical and userfriendly toxicity classification system with microbiotests for natural waters and wastewaters.*** *Environmental Toxicology*, 18(6), 395–402, 2003

[4]. The Commision on the Protection of the Black Sea Against Pollution, 2009. www.blacksea-commision.org/main.asp

For Authors

Are edited scientific papers in topics, written in English. Papers are selected after a peer review. Each participant is allowed to send maximum 2 papers as first author. Authors should make sure that the manuscripts submitted are ready for refereeing. The papers that are to be published must bring scientific contributions to the journal. The papers also have to contain the results of some of your work. It is strongly recommended an even number of pages, no longer than 6-10 pages. The papers that do not respect the publishing conditions and which are not integrated in the thematic of this journal will be rejected from the start by the Editorial Board. Authors submitting an article affirm that the same manuscript is not concurrently submitted to another publication. The authors are entirely responsible for the content of their papers.

PUBLISHED SINCE 2008
ISSN:1844-6116
ON LINE SINCE: 2008
PUBLISHED BY: Editura Nautica/ Constanta Maritime University